J. Fluid Mech. (1996), vol. 320, pp. 305–329

The second-order moment structure of dispersing plumes and puffs

By DAVID J. THOMSON

Meteorological Office, London Road, Bracknell, Berks RG12 2SZ, UK

(Received 30 December 1994 and in revised form 23 January 1996)

A description of the behaviour of the second-order moments of concentration for a variety of source types is derived within the context of the classical phenomenology of isotropic turbulence. The sources considered include instantaneous area, line and point sources and can also be interpreted as relating to plumes from continuous point sources and continuous crosswind line sources in a strong uniform mean flow. A large number of different regimes are identified corresponding to different relative sizes of the many length scales involved. Perhaps the most interesting result is the identification of an 'inertial–meander' subrange when the inertial-subrange eddies contribute to the meandering of the plume.

1. Introduction

Classical theory, as summarized by e.g. Monin & Yaglom (1975), has lead to a good phenomenological picture of the evolution of isotropic scalar fields in isotropic turbulence. In contrast the phenomenology of non-isotropic scalar fields is much less well understood; indeed the diversity of phenomena present may make it impossible to understand such flows in terms of a few universal concepts. Here we consider what is perhaps the next simplest class of flows after the class of isotropic flows, namely flows in which the velocity field is isotropic but in which the scalar field is non-isotropic as a result of the source configuration. More specifically we consider instantaneous area, line and point sources. The results for these sources can also be interpreted in the usual way as relating to plumes from continuous point sources and continuous crosswind line sources in flows with a strong uniform mean velocity. Consideration is restricted to the phenomenology of second-order moments (including two-point moments) at high Reynolds and Péclet numbers within the framework of classical theory (e.g. we ignore intermittency effects – this is probably acceptably accurate for second-order moments).

The main motivation for this study is derived from the dispersion of contaminants in the turbulent boundary layer of the atmosphere, although we hope the results may be of wider interest. Fluctuations in the concentration of atmospheric contaminants can be of considerable importance in the case of fast-acting toxic contaminants (see e.g. Griffiths & Megson 1984; Griffiths & Harper 1985; Griffiths 1991), inflammable substances or odours. Of course atmospheric flows are not isotropic or homogeneous – however in many atmospheric situations some of our results should be good approximations while in others we hope that, intelligently applied, the results should give qualitative insight.

Perhaps the main difficulty in extending the classical results to non-isotropic scalar

fields is the number of length scales of relevance to the problem. Excluding the microscales which we assume are much smaller than all other scales, the relevant scales for plumes and puffs include the source size, the turbulence integral scale, the root-mean-square displacement of particles at the time of interest, the root-mean-square separation of pairs of particles which are initially close, and, for two-point moments, the separation of the two points under consideration. Our approach here is to investigate systematically the behaviour of the two-point second-order moments in various subranges according to the relative sizes of these length scales.

We restrict consideration to situations with travel times much less than the turbulence integral time scale. This case is simpler than the situation for longer travel times and is also more useful since for such travel times most flows can be considered to be approximately homogeneous. (Although the analysis presented here assumes isotropy and not just homogeneity, it could be extended without great difficulty to homogeneous non-isotropic flows). Also we consider only length scales and travel times much longer than the length and time scales associated with the small-scale end of the inertial–convective subrange.

It is perhaps appropriate to comment on the relation of the ideas discussed here to the basic equations describing the problem, i.e. the Navier–Stokes, incompressibility and advection–diffusion equations. As is well known, it is in general impossible to make much progress from first principles starting from these equations – hence our use here of the classical phenomenology which is based on general principles but which, with a few exceptions, is not rigorously related to the underlying fluid dynamic equations and indeed probably cannot be so related (e.g. the classical picture ignores intermittency effects). The use of the classical phenomenology means we are restricted to obtaining results in a number of distinct regimes. The behaviour in the transitions between regimes could be obtained with models (such as the two-particle random walk model of Thomson 1990) – however the aim here is to achieve qualitative understanding rather than quantitative prediction and to obtain results which are not dependent on particular closure models.

2. Notation and framework for analysis

The starting point is the relation of the first and second moments of the contaminant concentration $c(\boldsymbol{x}, t)$ to the statistics of the motion of single particles and particle pairs. Here we take particles to be mathematical idealizations of molecules which are advected by the flow and also undergo a random molecular motion. With this definition two distinct particles can be coincident and particles which are coincident at one time can separate. Although this definition is important conceptually, the precise nature of the random motion is unimportant here because of our restriction to scales larger than the microscales. For further discussion of the role molecular diffusion in the motion of particle pairs and of possible definitions of what constitutes a 'particle' see e.g. Durbin (1980), Sawford & Hunt (1986) and Thomson (1990). Let $\boldsymbol{X}_1(t)$ and $\boldsymbol{X}_2(t)$ denote the trajectories of a pair of particles. The single-particle transition probability density function (p.d.f.), i.e. the p.d.f. of $\boldsymbol{X}_1(s)$ given $\boldsymbol{X}_1(t) = \boldsymbol{x}$, will be written $p_1(\boldsymbol{y}, s|\boldsymbol{x}, t)$ where $\boldsymbol{y}$ indicates a possible value for $\boldsymbol{X}_1(s)$. Similarly the two-particle transition p.d.f., i.e. the p.d.f. of $(\boldsymbol{X}_1(s), \boldsymbol{X}_2(s))$ given $(\boldsymbol{X}_1(t), \boldsymbol{X}_2(t)) = (\boldsymbol{x}_1, \boldsymbol{x}_2)$, will be written $p_2(\boldsymbol{y}_1, \boldsymbol{y}_2, s|\boldsymbol{x}_1, \boldsymbol{x}_2, t)$. Then, for an instantaneous source $S(\boldsymbol{y})$ at time s, we have, for $t > s$,

$$\langle c(\boldsymbol{x}, t)\rangle = \int p_1(\boldsymbol{y}, s|\boldsymbol{x}, t)\langle S(\boldsymbol{y})\rangle \, \mathrm{d}\boldsymbol{y} \tag{1}$$

and

$$\langle c(\boldsymbol{x}_1,t)c(\boldsymbol{x}_2,t)\rangle = \int p_2(\boldsymbol{y}_1,\boldsymbol{y}_2,s|\boldsymbol{x}_1,\boldsymbol{x}_2,t)\langle S(\boldsymbol{y}_1)S(\boldsymbol{y}_2)\rangle \,\mathrm{d}\boldsymbol{y}_1\,\mathrm{d}\boldsymbol{y}_2 \tag{2}$$

where $\langle\rangle$ indicates an ensemble average (see e.g. Durbin 1980; Sawford & Hunt 1986; Thomson 1990). Equations (1) and (2) are expressed in terms of probabilities associated with back trajectories of particles, but an equivalent formulation in terms of forward trajectories is also possible (Egbert & Baker 1984). Note that we are assuming throughout this paper that the flow is of constant density – equations (1) and (2) are not correct in variable-density flows (Thomson 1987, 1990).

It is sometimes convenient to express $\boldsymbol{X}_1$ and $\boldsymbol{X}_2$ in a manner related to the separation and centre of mass of the pair of particles. To this end we will write $\boldsymbol{X}_\Delta = (\boldsymbol{X}_1 - \boldsymbol{X}_2)/\sqrt{2}$ and $\boldsymbol{X}_\Sigma = (\boldsymbol{X}_1 + \boldsymbol{X}_2)/\sqrt{2}$. The two-particle transition p.d.f. can then be defined as the p.d.f. of $\boldsymbol{X}_\Delta(s)$ and $\boldsymbol{X}_\Sigma(s)$ given $\boldsymbol{X}_\Delta(t) = \boldsymbol{x}_\Delta$ and $\boldsymbol{X}_\Sigma(t) = \boldsymbol{x}_\Sigma$. Defined in this way the p.d.f. will be written, with a slight abuse of notation, as $p_2(\boldsymbol{y}_\Delta,\boldsymbol{y}_\Sigma,s|\boldsymbol{x}_\Delta,\boldsymbol{x}_\Sigma,t)$ (strictly speaking this is a different function from the p_2 introduced above). In general, when quantities with subscripts Δ, Σ, 1 and 2 appear in the same equation, they are to be interpreted as related by $(-)_\Delta = ((-)_1 - (-)_2)/\sqrt{2}$ and $(-)_\Sigma = ((-)_1 + (-)_2)/\sqrt{2}$.

It is useful to have a notation for the second moments of the transition p.d.f.s. We will use $\boldsymbol{S}_\Delta(s|\boldsymbol{x}_\Delta,t)$, $\boldsymbol{S}_\Sigma(s|\boldsymbol{x}_\Delta,t)$ and $\boldsymbol{S}_1(s|t)$ to denote the mean-square displacement tensors $\langle(\boldsymbol{X}_\Delta(s) - \boldsymbol{X}_\Delta(t)) \otimes (\boldsymbol{X}_\Delta(s) - \boldsymbol{X}_\Delta(t))\rangle$, $\langle(\boldsymbol{X}_\Sigma(s) - \boldsymbol{X}_\Sigma(t)) \otimes (\boldsymbol{X}_\Sigma(s) - \boldsymbol{X}_\Sigma(t))\rangle$ and $\langle(\boldsymbol{X}_1(s) - \boldsymbol{X}_1(t)) \otimes (\boldsymbol{X}_1(s) - \boldsymbol{X}_1(t))\rangle$ for particle pairs with $\boldsymbol{X}_\Delta(t) = \boldsymbol{x}_\Delta$ and $\boldsymbol{X}_\Sigma(t) = \boldsymbol{x}_\Sigma$. Note that, because of the homogeneity of the flow, $\boldsymbol{S}_\Delta$, $\boldsymbol{S}_\Sigma$ and $\boldsymbol{S}_1$ are independent of $\boldsymbol{x}_\Sigma$ and, because $\boldsymbol{S}_1$ depends only on the motion of single particles, $\boldsymbol{S}_1$ is independent of $\boldsymbol{x}_\Delta$. Also $\boldsymbol{S}_\Delta$, $\boldsymbol{S}_\Sigma$ and $\boldsymbol{S}_1$ satisfy the identity $\boldsymbol{S}_\Delta + \boldsymbol{S}_\Sigma = 2\boldsymbol{S}_1$. For $\boldsymbol{x}_\Delta = 0$ (and for all $\boldsymbol{x}_\Delta$ in the case of $\boldsymbol{S}_1$) these tensors are isotropic and their (Cartesian) diagonal components will be denoted by $\sigma_\Delta^2(s|t)$, $\sigma_\Sigma^2(s|t)$ and $\sigma_1^2(s|t)$. For more general $\boldsymbol{x}_\Delta$, it is useful to have a measure of the change in particle separation. For this purpose we define $d(s|\boldsymbol{x}_\Delta,t) = (\mathrm{tr}\,\boldsymbol{S}_\Delta(s|\boldsymbol{x}_\Delta,t)/3)^{1/2}$. In $\boldsymbol{S}_\Delta$, σ_Δ, d etc. the dependencies on s, t and $\boldsymbol{x}_\Delta$ will sometimes be suppressed if s is the source time, t is the measurement time and $\boldsymbol{x}_\Delta$ is the separation of two points for which we are considering the two-point moment of c.

Area, line and point sources with Gaussian cross-sections aligned with a chosen set of Cartesian coordinate axes will be considered. In order to treat these cases together, we introduce a parameter λ to indicate the dimensionality of the source ($\lambda = 1$, 2 or 3). For a vector $\boldsymbol{x}$, we will write $\hat{\boldsymbol{x}}$ for the λ-dimensional vector consisting of the last λ Cartesian components of $\boldsymbol{x}$ and will write $\tilde{\boldsymbol{x}}$ for the $(3-\lambda)$-dimensional vector consisting of the first $3-\lambda$ components. The idea behind this notation is that, once we have defined our sources, $\hat{\boldsymbol{x}}$ will indicate the 'cross-source' components of $\boldsymbol{x}$ while $\tilde{\boldsymbol{x}}$ will indicate the 'along-source' components. On occasion we will integrate with respect to $\tilde{\boldsymbol{x}}$ – we adopt the convention that this has no effect if $\lambda = 3$. For a rank-two tensor $\boldsymbol{S}$, $\hat{\boldsymbol{S}}$ will denote the λ-dimensional sub-tensor defined in our chosen set of Cartesian coordinates by

$$\hat{\boldsymbol{S}} = \begin{cases} \boldsymbol{S} & \text{if } \lambda = 3 \\ \begin{pmatrix} S^{22} & S^{23} \\ S^{32} & S^{33} \end{pmatrix} & \text{if } \lambda = 2 \\ S^{33} & \text{if } \lambda = 1. \end{cases}$$

If $\boldsymbol{x}$ and $\boldsymbol{S}$ are a λ-dimensional vector and tensor, $\mathscr{G}_\lambda(\boldsymbol{x},\boldsymbol{S})$ will denote the λ-

dimensional Gaussian distribution with covariance tensor $\boldsymbol{S}$. $\mathscr{G}_\lambda(\boldsymbol{x}, \sigma^2)$ will be used to denote $\mathscr{G}_\lambda(\boldsymbol{x}, \sigma^2 \hat{\boldsymbol{I}})$ where $\boldsymbol{I}$ is the tensor with Cartesian components equal to the identity matrix. Occasionally we will write $\mathscr{G}_\lambda(\boldsymbol{x}, \boldsymbol{S})$ and $\mathscr{G}_\lambda(\boldsymbol{x}, \sigma^2)$ with $\boldsymbol{x}$ and/or $\boldsymbol{S}$ being three-dimensional; this is a shorthand for $\mathscr{G}_\lambda(\hat{\boldsymbol{x}}, \hat{\boldsymbol{S}})$ and $\mathscr{G}_\lambda(\hat{\boldsymbol{x}}, \sigma^2)$. The area, line and point sources can now be expressed as $S(\boldsymbol{y}) = \mathscr{G}_\lambda(\boldsymbol{y}, \sigma_0^2)$ where σ_0 is a measure of source size. Although we are not considering continuous sources explicitly, results at a downwind distance x for plumes from continuous point sources and continuous crosswind line sources in a strong uniform mean flow U can be regarded in the usual way as corresponding to results for dispersion from instantaneous line and area sources at time x/U after release. Provided the turbulence intensity is small this should be a reasonable approximation (see e.g. Townsend 1954).

It is also useful to consider homogeneous random sources (i.e. sources where the source strength, and hence the initial concentration field, is a random function which is homogeneous in space) with Gaussian correlation functions. Although such sources are well understood, the results are useful in studying the area, line and point sources. For such sources we have $\langle S(\boldsymbol{y}) \rangle = 0$ and $\langle S(\boldsymbol{y}_1) S(\boldsymbol{y}_2) \rangle = \mathscr{G}_\lambda(\boldsymbol{y}_\Delta, \sigma_0^2)$. This corresponds to an initial correlation function given by $\langle c(\boldsymbol{y}_1, s) c(\boldsymbol{y}_2, s) \rangle = \mathscr{G}_\lambda((\boldsymbol{y}_1 - \boldsymbol{y}_2)/\sqrt{2}, \sigma_0^2)$.

We will also consider linear sources (i.e. sources where the source strength varies linearly in space – not to be confused with line sources). As for the homogeneous random sources, the results for these sources are useful in studying the area, line and point sources. For such sources we have $S(\boldsymbol{y}) = \hat{\boldsymbol{y}}$ with $\lambda = 1$.

Because we are sometimes interested in small differences (such as $\langle c(\boldsymbol{x}, t)^2 \rangle - \langle c(\boldsymbol{x}, t) \rangle^2$ near the source or the departure of $\langle c(\boldsymbol{x}_1, t) c(\boldsymbol{x}_2, t) \rangle$ from $\langle c((\boldsymbol{x}_1 + \boldsymbol{x}_2)/2, t)^2 \rangle$ for small values of $|\boldsymbol{x}_1 - \boldsymbol{x}_2|$) we will need to keep track of the size of errors in the analysis. For this purpose we use the usual mathematical notations $O(a)$ and $o(a)$ to denote quantities of order a and quantities which are much smaller than a respectively. Precise definitions of O and o are given in Appendix A. The notation $+o$ is used to indicate 'plus asymptotically smaller terms'; for example, in $A + B(C + (D + E) + o)$, o denotes terms which are $o(C)$ and $o(D + E)$. As indicated in §1 we consider only the classical phenomenology (e.g. we ignore intermittency effects) and our error estimates reflect only those errors which would be present even if the classical view was exact or which are introduced by approximations which are made in the mathematical analysis. The error estimates do not account for errors in the classical picture or indeed for errors introduced by the approximations made in §3 below.

In the two-point moments, we adopt the convention that quantities such as $\boldsymbol{x}$, $\langle c \rangle$ and $\langle c^2 \rangle$ refer to values at the point midway between the two points being considered, i.e. at $(\boldsymbol{x}_1 + \boldsymbol{x}_2)/2$; $\langle cc \rangle$ and $\langle c \rangle \langle c \rangle$ however denote products of values at $\boldsymbol{x}_1$ and $\boldsymbol{x}_2$. $\langle c(0) \rangle$ denotes $\langle c \rangle$ at $\boldsymbol{x} = 0$.

Throughout the following we take the flow to be isotropic turbulence with velocity variance σ_v^2, energy dissipation rate ε and integral length and time scales L and τ, with τ being of order L/σ_v and ε being of order σ_v^3/L or σ_v^2/τ.

3. Sawford's approximation

The approximation introduced by Sawford (1983) plays a central role in the analysis presented in this paper. Sawford approximated $p_2(\boldsymbol{y}_\Delta, \boldsymbol{y}_\Sigma, s | \boldsymbol{x}_\Delta, \boldsymbol{x}_\Sigma, t)$ by

$$\mathscr{G}_3(\boldsymbol{y}_\Sigma - \boldsymbol{x}_\Sigma, \boldsymbol{S}_\Sigma(s | \boldsymbol{x}_\Delta, t)) p_\Delta(\boldsymbol{y}_\Delta, s | \boldsymbol{x}_\Delta, t) \tag{3}$$

where $p_\Delta(\boldsymbol{y}_\Delta, s | \boldsymbol{x}_\Delta, t)$ is the p.d.f. of $\boldsymbol{X}_\Delta(s)$ given $\boldsymbol{X}_\Delta(t) = \boldsymbol{x}_\Delta$ (in fact Sawford only considered the case $\boldsymbol{x}_\Delta = 0$ and (3) above is an extension of his original proposal

to more general values of $\boldsymbol{x}_\Delta$). The assumptions involved in this are that $\boldsymbol{X}_\Sigma(s)$ is Gaussian (which is certainly a reasonable approximation) and that, for fixed $\boldsymbol{X}_\Delta(t)$, $\boldsymbol{X}_\Delta(s)$ and $\boldsymbol{X}_\Sigma(s)$ are independent. The accuracy of the latter assumption is not so clear, although the assumption is supported by the fact that $\boldsymbol{X}_\Delta(s)$ and $\boldsymbol{X}_\Sigma(s)$ are uncorrelated. Further support comes, when $\boldsymbol{X}_\Delta(t)$ is small and $|t-s| \ll \tau$, from the idea that the small and large eddies (which dominate the evolution of $\boldsymbol{X}_\Delta$ and $\boldsymbol{X}_\Sigma$ respectively) are quasi-independent and, when $\boldsymbol{X}_\Delta(t)$ is large or $|t-s| \gg \tau$, from the fact that the particles move approximately independently with Gaussian displacements (see Batchelor 1952). In conjunction with Sawford's approximation it is natural to assume that p_1 is Gaussian, i.e.

$$p_1(\boldsymbol{y}, s|\boldsymbol{x}, t) = \mathscr{G}_3(\boldsymbol{y}-\boldsymbol{x}, \sigma_1^2(s|t)). \tag{4}$$

Again this is certainly a reasonably accurate approximation (see e.g. Monin & Yaglom 1971, §9.3).

Unfortunately Sawford's approximation (3) cannot be exact for both $t > s$ and $t < s$ because it violates the principle that $p_2(\boldsymbol{y}_\Delta, \boldsymbol{y}_\Sigma, s|\boldsymbol{x}_\Delta, \boldsymbol{x}_\Sigma, t) = p_2(\boldsymbol{x}_\Delta, \boldsymbol{x}_\Sigma, t|\boldsymbol{y}_\Delta, \boldsymbol{y}_\Sigma, s)$. However, although it is unlikely to be exact, (3) does not appear to violate any fundamental constraints if, as in the use we make of it below, it is only assumed for $t > s$. The symmetry of (3) could be improved by replacing $\boldsymbol{S}_\Sigma(s|\boldsymbol{x}_\Delta, t)$ by $(\boldsymbol{S}_\Sigma(t|\boldsymbol{y}_\Delta, s) + \boldsymbol{S}_\Sigma(s|\boldsymbol{x}_\Delta, t))/2$. Provided p_Δ satisfies the exact result that $p_\Delta(\boldsymbol{y}_\Delta, s|\boldsymbol{x}_\Delta, t) = p_\Delta(\boldsymbol{x}_\Delta, t|\boldsymbol{y}_\Delta, s)$, then the modified form for p_2 does satisfy the principle. However it can be shown that the modified form cannot be exactly correct either since it leads to at least one of $\boldsymbol{S}_\Sigma(t|\boldsymbol{y}_\Delta, s)$ and $\boldsymbol{S}_\Sigma(s|\boldsymbol{x}_\Delta, t)$ as calculated from the modified equation (3) being unequal to the value assumed in defining p_2. A consequence of this is that (at least if the value of $\boldsymbol{S}_\Sigma$ used in defining p_2 satisfies $\boldsymbol{S}_\Delta + \boldsymbol{S}_\Sigma = 2\boldsymbol{S}_1$) the mean square of $\int c(\boldsymbol{x}, t)R(\boldsymbol{x})\,\mathrm{d}\boldsymbol{x}$ as calculated from $\langle c(\boldsymbol{x}_1, t)c(\boldsymbol{x}_2, t)\rangle$ using (2) and the modified equation (3) can, for some choices of R and S, be less than the square of the mean calculated from (1). Hence it seems that symmetrizing (3) makes matters worse rather than better (as well as making deductions about concentration fluctuations much more difficult). In addition to these problems, (3) is not exactly consistent with (4) unless p_Δ is Gaussian. However, despite these problems, it seems likely that the approximations (3) and (4) are reasonably accurate in many situations. This view is supported partly by previous uses of the approximations (e.g. Thomson 1990) and partly by the discussion in §5 where the sensitivity of the results to the Sawford approximation is investigated.

Using (3) and (4) we obtain

$$\langle c(\boldsymbol{x}, t)\rangle = \mathscr{G}_\lambda(\boldsymbol{x}, \sigma_0^2 + \sigma_1^2) \tag{5}$$

and

$$\langle c(\boldsymbol{x}_1, t)c(\boldsymbol{x}_2, t)\rangle = \mathscr{G}_\lambda(\boldsymbol{x}_\Sigma, \sigma_0^2\boldsymbol{I} + \boldsymbol{S}_\Sigma(s|\boldsymbol{x}_\Delta, t)) \int p_\Delta(\boldsymbol{y}_\Delta, s|\boldsymbol{x}_\Delta, t)\mathscr{G}_\lambda(\boldsymbol{y}_\Delta, \sigma_0^2)\,\mathrm{d}\boldsymbol{y}_\Delta \tag{6}$$

for the area, line and point sources. For the homogeneous random sources we have (without needing to use the Sawford approximation) $\langle c(\boldsymbol{x}, t)\rangle = 0$ and

$$\langle c(\boldsymbol{x}_1, t)c(\boldsymbol{x}_2, t)\rangle = \int p_\Delta(\boldsymbol{y}_\Delta, s|\boldsymbol{x}_\Delta, t)\mathscr{G}_\lambda(\boldsymbol{y}_\Delta, \sigma_0^2)\,\mathrm{d}\boldsymbol{y}_\Delta. \tag{7}$$

The study of the homogeneous source case is useful in understanding the area, line and point sources for two reasons. Firstly the integral in (7) also occurs in the result for area, line and point sources (equation (6)). Also, for fixed $\boldsymbol{x}_\Delta$, the spatial

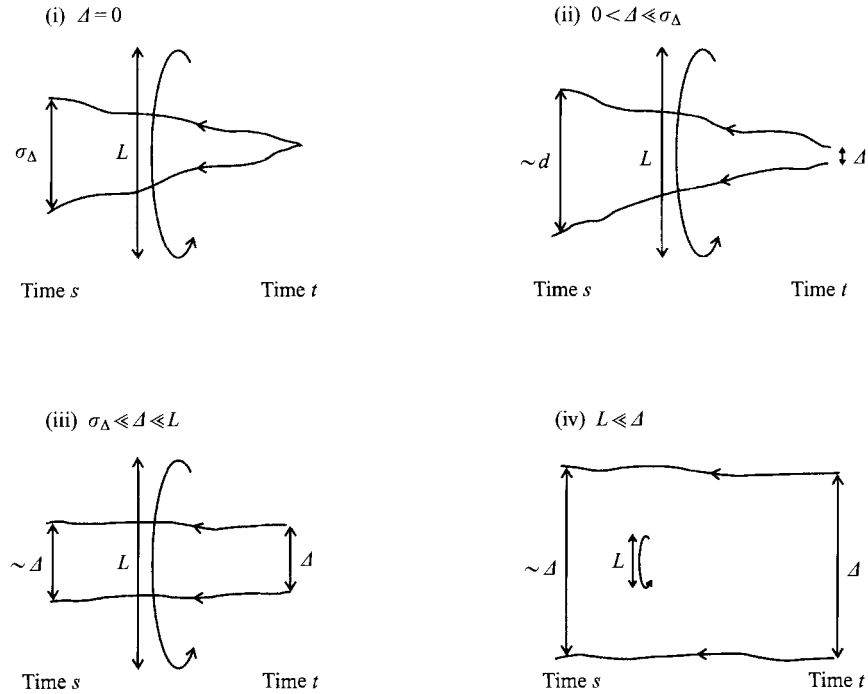

FIGURE 1. Schematic illustration of the motion of particle pairs. Backwards trajectories are shown from time t to time s ($s < t$, $t - s \ll \tau$) for various separations at time t. The scale L of the energy-containing eddies is also shown.

integral of $\langle c(\boldsymbol{x}_1, t)c(\boldsymbol{x}_2, t)\rangle$ for the area, line and point sources (more precisely the integral $\int \langle c(\boldsymbol{x}_1, t)c(\boldsymbol{x}_2, t)\rangle \, \mathrm{d}\hat{\boldsymbol{x}}_\Sigma$) equals $\langle c(\boldsymbol{x}_1, t)c(\boldsymbol{x}_2, t)\rangle$ for the homogeneous random sources (and this result is independent of the Sawford approximation). For the linear sources ($\lambda = 1$) we have (again without needing to use the Sawford approximation) $\langle c(\boldsymbol{x}, t)\rangle = \hat{\boldsymbol{x}}$ and

$$\langle c'(\boldsymbol{x}_1, t)c'(\boldsymbol{x}_2, t)\rangle = \sigma_1^2(s|t) - \hat{\boldsymbol{S}}_\Delta(s|\boldsymbol{x}_\Delta, t) \tag{8}$$

where $c' = c - \langle c\rangle$. For the linear sources we consider $\langle c'(\boldsymbol{x}_1, t)c'(\boldsymbol{x}_2, t)\rangle$ rather than $\langle c(\boldsymbol{x}_1, t)c(\boldsymbol{x}_2, t)\rangle$ since, by subtracting the mean concentration, we obtain two-point moments which depend only on the separation of the two points. The study of the linear source case is useful in understanding the area, line and point sources in situations where the latter sources can be approximated by linear functions.

4. Transition probabilities

To apply equations (5) to (8) we need to determine $\sigma_1^2(s|t)$ and $p_\Delta(\boldsymbol{y}_\Delta, s|\boldsymbol{x}_\Delta, t)$ for $t > s$. $\boldsymbol{S}_\Sigma(s|\boldsymbol{x}_\Delta, t)$, which is needed in (6), can then be determined from $\boldsymbol{S}_\Delta + \boldsymbol{S}_\Sigma = 2\sigma_1^2\boldsymbol{I}$. The behaviour of $\sigma_1^2(s|t)$ is straightforward. Since we are assuming $t - s \ll \tau$, $\sigma_1^2(s|t)$ can be calculated by assuming that the particles travel in straight lines to leading order, giving $\sigma_1^2(s|t) = \sigma_v^2(t-s)^2 + o$ (Monin & Yaglom 1971, p. 540). The behaviour of p_Δ is more complicated. However its qualitative behaviour is well understood classically (see e.g. Monin & Yaglom 1975, §24). In the following we summarize the classical results in a form appropriate for our present purposes.

We will consider $p_\Delta(\boldsymbol{y}_\Delta, s|\boldsymbol{x}_\Delta, t)$ with $\boldsymbol{x}_\Delta$ fixed and, writing Δ for $|\boldsymbol{x}_\Delta|$, will consider

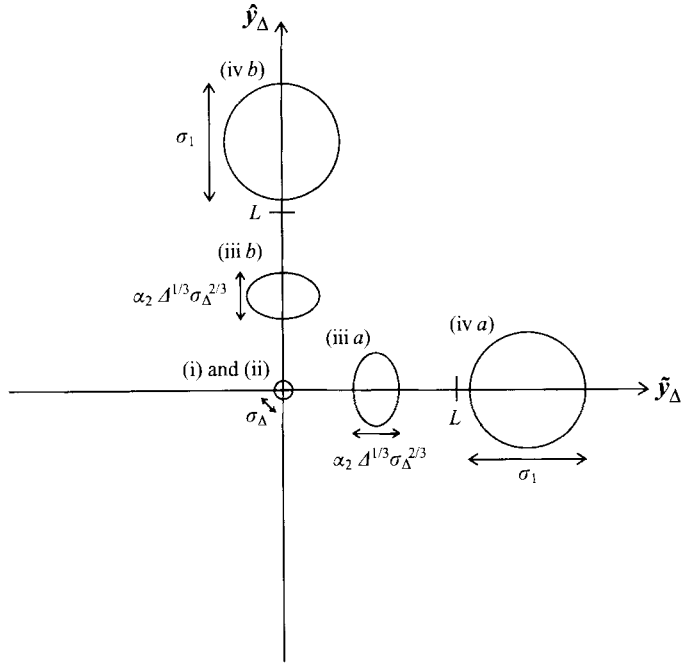

FIGURE 2. Schematic illustration of $\int p_\Delta(\boldsymbol{y}_\Delta, s|\boldsymbol{x}_\Delta, t)\,\mathrm{d}\tilde{y}$ for $\hat{y}_\Delta = 0$. The extent of the distribution $p_\Delta(\boldsymbol{y}_\Delta, s|\boldsymbol{x}_\Delta, t)$ (i.e. the region where $p_\Delta(\boldsymbol{y}_\Delta, s|\boldsymbol{x}_\Delta, t)$ is significantly non-zero) is shown for various values of $\boldsymbol{x}_\Delta$: (i) and (ii) denote the cases $\Delta = 0$ and $0 < \Delta \ll \sigma_\Delta$, (iii$a$) and (iii$b$) denote $\sigma_\Delta \ll \Delta \ll L$ with $\hat{x}_\Delta = 0$ and $\tilde{x}_\Delta = 0$ respectively, and (iv$a$) and (iv$b$) denote $L \ll \Delta$ with $\hat{x}_\Delta = 0$ and $\tilde{x}_\Delta = 0$ respectively. $\hat{x}_\Delta = 0$ implies that $\boldsymbol{x}_\Delta$ lies in the along-source direction while $\tilde{x}_\Delta = 0$ implies that $\boldsymbol{x}_\Delta$ lies in the across-source direction. The integral is evaluated along the line $\hat{y}_\Delta = 0$. Using the figure, one can see the extent to which the region of integration intercepts the region where $p_\Delta(\boldsymbol{y}_\Delta, s|\boldsymbol{x}_\Delta, t)$ is significantly non-zero.

the different regimes corresponding to $\Delta = 0$, $0 < \Delta \ll \sigma_\Delta$, $\sigma_\Delta \ll \Delta \ll L$ and $L \ll \Delta$. For all these regimes the mean of the distribution is of course $\boldsymbol{x}_\Delta$. The behaviour of particle pairs in each of these regimes is depicted schematically in figure 1. For each regime we also consider the behaviour of $\int p_\Delta(\boldsymbol{y}_\Delta, s|\boldsymbol{x}_\Delta, t)\,\mathrm{d}\tilde{y}_\Delta$ for $\hat{y}_\Delta = 0$. This quantity is of interest because of its role in (6) and (7) in the limit of small σ_0 (in this limit S is concentrated at $\hat{y}_\Delta = 0$). The integral is illustrated schematically in figure 2.

(i) $\Delta = 0$: The classical Richardson law gives $\sigma_\Delta^2 = \alpha\varepsilon(t-s)^3 + o$ for some constant α. Since the statistics of concentration depend mainly on the sizes of the various length scales, the relation $\sigma_\Delta^2 = \alpha\varepsilon(t-s)^3 + o$ will often be used to re-express time in terms of σ_Δ. The classical theory implies that p_Δ is isotropic and is more peaked than Gaussian, and that it grows self-similarly to leading order. (In fact the leading-order self-similarity is probably only true for $|\boldsymbol{y}_\Delta| \not\gg \sigma_\Delta$. In the extreme tails, small changes such as the departure of σ_Δ^2 from $\alpha\varepsilon(t-s)^3$ which results from the fact that τ is not infinitely large in relation to $t-s$ may have large effects.) $\boldsymbol{S}_\Delta$ and d are given by $\boldsymbol{S}_\Delta = \sigma_\Delta^2 \boldsymbol{I}$ and $d = \sigma_\Delta$. For $\hat{y}_\Delta = 0$ we can write $\int p_\Delta(\boldsymbol{y}_\Delta, s|\boldsymbol{x}_\Delta, t)\,\mathrm{d}\tilde{y}_\Delta = \mu_i \mathscr{G}_i(0, \sigma_\Delta^2) + o$ where the μ_i are constants reflecting the non-Gaussianity (see (i) in figure 2). Because the integration tends to smooth out the peakiness of p_Δ we expect $\mu_3 > \mu_2 > \mu_1 > 1$.

(ii) $0 < \Delta \ll \sigma_\Delta$: For this case the results in the previous paragraph are a good approximation. However we need to consider the leading-order correction to the picture in the preceeding paragraph which results from the non-zero value of Δ. We

use Batchelor's (1952) argument that p_Δ almost forgets the 'initial' separation Δ, the effect of non-zero Δ being, to leading order, simply a shift in the time origin by an amount of order $\Delta^{2/3}/\varepsilon^{1/3}$. This implies p_Δ has the same shape as for $\Delta = 0$ but with $\boldsymbol{S}_\Delta = \sigma_\Delta^2(1 + \alpha_1\Delta^{2/3}/\sigma_\Delta^{2/3})^2\boldsymbol{I} + o(\Delta^{2/3}\sigma_\Delta^{4/3})$ and $d = \sigma_\Delta(1 + \alpha_1\Delta^{2/3}/\sigma_\Delta^{2/3} + o)$ for some constant α_1. Note that this 'time-advanced' p_Δ has the wrong mean (zero instead of $\boldsymbol{x}_\Delta$); however, because $\Delta \ll d - \sigma_\Delta$, any correction of this will have a much smaller effect than the time advancement, confirming that the time advancement does give the leading-order correction for the effect of non-zero Δ. For $\hat{\boldsymbol{y}}_\Delta = 0$ we have that $\int p_\Delta(\boldsymbol{y}_\Delta, s|\boldsymbol{x}_\Delta, t)\,\mathrm{d}\tilde{\boldsymbol{y}}_\Delta$ equals the value at $\Delta = 0$ times $(1 - \lambda\alpha_1\Delta^{2/3}/\sigma_\Delta^{2/3} + o)$ (see (ii) in figure 2). For $\lambda = 3$ we have $p_\Delta(0, s|\boldsymbol{x}_\Delta, t) = p_\Delta(0, s|0, t)(1 - 3\alpha_1\Delta^{2/3}/\sigma_\Delta^{2/3} + o)$, showing that $p_\Delta(0, s|\boldsymbol{x}_\Delta, t)$ is peaked at $\boldsymbol{x}_\Delta = 0$. The same argument with $\boldsymbol{y}_\Delta$ fixed instead of $\boldsymbol{x}_\Delta$ supports the peaked nature of $p_\Delta(\boldsymbol{y}_\Delta, s|0, t)$ mentioned in the previous paragraph. α_1 can be related to the Obukhov–Corrsin constant in the inertial-subrange structure function for scalars by considering a random isotropic source with $\langle S(\boldsymbol{y}_1)S(\boldsymbol{y}_2)\rangle = \delta(\boldsymbol{y}_\Delta)$. This gives $\langle c^2\rangle = \mu_3\mathscr{G}_3(0, \sigma_\Delta^2) + o$ and $\langle cc\rangle = \langle c^2\rangle(1 - 3\alpha_1\Delta^{2/3}/\sigma_\Delta^{2/3} + o)$ and the rate of dissipation of $\langle c^2\rangle/2$, ε_c, is given by

$$\varepsilon_c = -\frac{1}{2}\frac{\mathrm{d}\langle c^2\rangle}{\mathrm{d}t} = -\frac{1}{2}\langle c^2\rangle\sigma_\Delta^3\frac{\mathrm{d}\sigma_\Delta^{-3}}{\mathrm{d}t} = \frac{9\langle c^2\rangle}{4(t-s)} = \frac{9\langle c^2\rangle\alpha^{1/3}\varepsilon^{1/3}}{4\sigma_\Delta^{2/3}}.$$

It follows that $\langle cc\rangle = \langle c^2\rangle - (4\alpha_1/3\alpha^{1/3})\varepsilon_c\varepsilon^{-1/3}\Delta^{2/3}$ and hence that $C_\theta = 2^{8/3}\alpha_1/3\alpha^{1/3}$ where C_θ is the Obukhov–Corrsin constant (as defined by Monin & Yaglom 1975, p. 384). It is interesting to note that the inertial-subrange form for the scalar structure function follows from the assumption that the effect of non-zero Δ can be represented by a shift in the time origin of the separation process. In fact the shift in time can be written in terms of C_θ as $C_\theta\Delta^{2/3}/2^{5/3}\varepsilon^{1/3}$.

(iii) $\sigma_\Delta \ll \Delta \ll L$: In this regime we have $t - s \ll \Delta^{2/3}/\varepsilon^{1/3}$ and so we can assume that the particles travel in straight lines to leading order. From our understanding of the two-point velocity p.d.f. for separations lying in the inertial subrange, it follows that p_Δ is non-isotropic and non-Gaussian and, viewed in a frame aligned with $\boldsymbol{x}_\Delta$, the shape of p_Δ is independent of $\boldsymbol{x}_\Delta$ and t to leading order (at least for $|\boldsymbol{y}_\Delta - \boldsymbol{x}_\Delta| \not\gg d$). $\boldsymbol{S}_\Delta$ is given by

$$\boldsymbol{S}_\Delta = \tfrac{1}{2}C\varepsilon^{2/3}(\Delta\sqrt{2})^{2/3}(t-s)^2\left(\tfrac{4}{3}\boldsymbol{I} - \frac{1}{3}\frac{\boldsymbol{x}_\Delta \otimes \boldsymbol{x}_\Delta}{\Delta^2}\right) + o = \alpha_2\Delta^{2/3}\sigma_\Delta^{4/3}\left(\tfrac{4}{3}\boldsymbol{I} - \frac{1}{3}\frac{\boldsymbol{x}_\Delta \otimes \boldsymbol{x}_\Delta}{\Delta^2}\right) + o$$

where C is the inertial-subrange constant in the longitudinal structure function (as defined by Monin & Yaglom 1975, p. 353) and $\alpha_2 = C/(2\alpha)^{2/3}$. It follows that $d = ((11/9)\alpha_2)^{1/2}\Delta^{1/3}\sigma_\Delta^{2/3} + o$. For $\hat{\boldsymbol{y}}_\Delta = 0$ and $\hat{\boldsymbol{x}}_\Delta = 0$ (and so $|\tilde{\boldsymbol{x}}_\Delta| = \Delta$) we can write $\int p_\Delta(\boldsymbol{y}_\Delta, s|\boldsymbol{x}_\Delta, t)\,\mathrm{d}\tilde{\boldsymbol{y}}_\Delta = v_\lambda\mathscr{G}_\lambda(0, \alpha_2\Delta^{2/3}\sigma_\Delta^{4/3}) + o$ where the v_λ account for the anisotropy and non-Gaussianity in p_Δ (see (iii*a*) in figure 2). Note that this result only applies for $\lambda = 1$ or 2; for $\lambda = 3$ we have $\hat{\boldsymbol{x}}_\Delta = \boldsymbol{x}_\Delta$ and so $\hat{\boldsymbol{x}}_\Delta = 0$ implies $\Delta = 0$, violating $\sigma_\Delta \ll \Delta$. For $\hat{\boldsymbol{y}}_\Delta = 0$ and $|\hat{\boldsymbol{x}}_\Delta| \gg \Delta^{1/3}\sigma_\Delta^{2/3}$ the particles with $\boldsymbol{X}_\Delta(t) = \boldsymbol{x}_\Delta$ cannot easily reach $\hat{\boldsymbol{y}}_\Delta = 0$ and so $\int p_\Delta(\boldsymbol{y}_\Delta, s|\boldsymbol{x}_\Delta, t)\,\mathrm{d}\tilde{\boldsymbol{y}}_\Delta$ is very small (see (iii*b*) in figure 2).

(iv) $L \ll \Delta$: As in the previous case, we can assume that the particles travel in straight lines to leading order; however, unlike the previous case we can also assume the particles move independently. Hence, using (4), we can take p_Δ to be Gaussian and isotropic to leading order (at least for $|\boldsymbol{y}_\Delta - \boldsymbol{x}_\Delta| \not\gg \sigma_1$) with $\boldsymbol{S}_\Delta = \sigma_1^2\boldsymbol{I} + o$ and $d = \sigma_1 + o$. For $\hat{\boldsymbol{y}}_\Delta = 0$ and $|\hat{\boldsymbol{x}}_\Delta| \not\gg \sigma_1$ (as in (iii) above this can only happen for $\lambda = 1$ or 2) we have $\int p_\Delta(\boldsymbol{y}_\Delta, s|\boldsymbol{x}_\Delta, t)\,\mathrm{d}\tilde{\boldsymbol{y}}_\Delta = \mathscr{G}_\lambda(\boldsymbol{x}_\Delta, \sigma_1^2) + o$ (see (iv*a*) in figure 2) while

for $\hat{\boldsymbol{y}}_\Delta = 0$ and $|\hat{\boldsymbol{x}}_\Delta| \gg \sigma_1$ we have that $\int p_\Delta(\boldsymbol{y}_\Delta, s|\boldsymbol{x}_\Delta, t)\,\mathrm{d}\tilde{\boldsymbol{y}}_\Delta$ is very small (see (iv*b*) in figure 2).

In fact the idea that particles travel in straight lines to leading order is valid for all $\Delta \gg \sigma_\Delta$. Hence, if we knew the velocity structure function $\boldsymbol{D}(\boldsymbol{x}_1 - \boldsymbol{x}_2)$ (defined as $\langle(\boldsymbol{u}(\boldsymbol{x}_1) - \boldsymbol{u}(\boldsymbol{x}_2)) \otimes (\boldsymbol{u}(\boldsymbol{x}_1) - \boldsymbol{u}(\boldsymbol{x}_2))\rangle$ where $\boldsymbol{u}$ is the velocity field), we could obtain an expression for $\boldsymbol{S}_\Delta$ which is valid for all such Δ, namely $\boldsymbol{S}_\Delta = \frac{1}{2}\boldsymbol{D}(\boldsymbol{x}_1 - \boldsymbol{x}_2)(t-s)^2 + o$. Similarly, if we knew the relative velocity p.d.f. we could calculate p_Δ to leading order for all $\Delta \gg \sigma_\Delta$.

For all the above cases it is generally assumed classically that all moments of p_Δ exist; indeed this seems almost certain to be true in view of the difficulty of generating extremely large velocities.

Note there is no particular reason why $p_\Delta(\boldsymbol{y}_\Delta, s|\boldsymbol{x}_\Delta, t)$ should equal $p_\Delta(\boldsymbol{y}_\Delta, t|\boldsymbol{x}_\Delta, s)$ (although it does equal $p_\Delta(\boldsymbol{x}_\Delta, t|\boldsymbol{y}_\Delta, s)$ as discussed in §3 above), and in fact the lack of time-reversal symmetry in turbulence (in particular the skewness of the distribution of two-point velocity differences for inertial-subrange separations) means that these quantities are not identical. Hence the forward dispersion version of p_Δ will be quantitatively (but not qualitatively) different from the reverse dispersion version discussed above (for example particles coincident at time t and followed backwards to time s will have a different root-mean-square spread to particles coincident at time s and followed forward to time t). An exception to this is p_Δ for $\sigma_\Delta \ll \Delta$. Here the shape of p_Δ is the same as the two-point relative velocity p.d.f. to leading order (except possibly in the extreme tails), and so the forward and reverse dispersion versions are the same to leading order. In particular the forward and reverse dispersion versions of v_1 and v_2 are equal.

Without attempting to be comprehensive, we will briefly discuss the values of the various constants defined above. The values of the constants C and C_θ are fairly well established from observations. Lesieur (1987, pp. 88 and 154) gives values for the spectral versions of the constants which correspond to $C \simeq 2.0$ and $C_\theta \simeq 3.2$. These values are consistent with those given by Monin & Yaglom (1975, pp. 485 and 504). The remaining constants are rather less well known. Consider first the constants which are relevant for $0 \leqslant \Delta \ll \sigma_\Delta$, namely α, α_1 and the μ_i. There is little reliable experimental evidence on these constants and so we will consider model results, in particular the results of Thomson's (1990) 'random walk' simulations and results from the eddy-damped quasi-normal Markovian (EDQNM) approximation obtained by Larchevêque & Lesieur (1981) (see also Lesieur 1987). Using model results is of course less satisfactory than using good quality experimental data would be and the results should not be viewed with any great confidence. However we note that the models in question have shown reasonable agreement with some experimental data on the second-order moments of concentration (Larchevêque *et al.* 1980; Herring *et al.* 1982; Lesieur 1987; Thomson 1990) and so the results should be useful in predicting the order of magnitude of the constants. Thomson's model assumes the flow field to be Gaussian and so gives the same value for the forward and reverse dispersion versions of p_Δ. In principle EDQNM could give different values for forward and reverse dispersion with the reverse dispersion form of p_Δ being calculated by varying the initial separation and using the result $p_\Delta(\boldsymbol{y}_\Delta, s|\boldsymbol{x}_\Delta, t) = p_\Delta(\boldsymbol{x}_\Delta, t|\boldsymbol{y}_\Delta, s)$. However it seems likely that any such differences are an artifact of the model (the EDQNM equations for p_Δ involve only the second-order velocity moments and so do not seem capable of correctly accounting for the lack of time-reversal symmetry in the turbulence). In any case, Larchevêque & Lesieur set one of EDQNM's adjustable constants to zero (as is usual in EDQNM) and approximate the damping time scales by their

asymptotic large-time form; this approximation yields a diffusion equation for p_Δ with the diffusivity depending on $\boldsymbol{x}_\Delta$ alone (and proportional to $|\boldsymbol{x}_\Delta|^{4/3}$ as in Richardson 1926) and so leads to identical predictions for the forward and reverse versions of p_Δ. The 'random walk' model simulations of Thomson (1990) give $\alpha \simeq 0.33$ and $\alpha_1 \simeq 0.56$ when the inertial subrange constant C_0 in the Lagrangian velocity structure function is set to 4.0, while EDQNM gives $\alpha \simeq 0.57$ and $\alpha_1 \simeq 1.3$ when tuned to give $C_\theta \simeq 3.2$ (Larchevêque & Lesieur 1981). Using $C_\theta = 2^{8/3}\alpha_1/3\alpha^{1/3}$, the random walk results imply $C_\theta \simeq 1.7$ which is almost certainly too low. Note also that, as pointed out by Kraichnan (1966), the use of the large-time approximation for the damping time scales in the EDQNM approximation is likely to lead to an overprediction of α_1 and hence, for fixed C_θ, of α. For μ_λ, Thomson's (1990) simulations (again with $C_0 = 4.0$) yield values of 1.4, 2.8 and 12 for $\lambda = 1$, 2 and 3, while EDQNM (with the large-time approximation for the damping time scales) gives the Richardson form $p_\Delta \propto \exp(-A\Delta^{2/3})$ (Lesieur 1987, p. 160; Monin & Yaglom 1975, p. 574) and yields values of 1.6, 4.1 and 28 for $\lambda = 1$, 2 and 3. We will now consider the constants which are relevant for $\sigma_\Delta \ll \Delta \ll L$, namely α_2, v_1 and v_2. α_2 is simply related to C and α which have been discussed above. v_1 and v_2 depend on the shape of p_Δ and, for the regime in question (i.e. $\sigma_\Delta \ll \Delta \ll L$), p_Δ has the same shape as the two-point relative velocity p.d.f. Hence, in principle, v_1 and v_2 could be determined from measurements of this p.d.f. If p_Δ were Gaussian, v_1 and v_2 would equal $\sqrt{3/4}$ and 3/4 respectively. The model used by Thomson (1990) and EDQNM (this time without the large-time approximation for the damping time scales – this approximation makes no sense in calculating v_1 and v_2) predict (incorrectly) p_Δ to be Gaussian for $\sigma_\Delta \ll \Delta \ll L$. In the case of Thomson (1990), this is because the two-point Eulerian velocity distributions are assumed Gaussian and, as noted above, we are concerned with a regime where p_Δ has the same shape as the two-point velocity p.d.f. Hence these models also give the Gaussian values for v_1 and v_2.

5. Second-order moments

From the above ideas we can obtain expressions for the second-order moments. The analysis is quite straightforward although somewhat lengthy because of the number of regimes which need to be considered. The central difficulty is in evaluating the integral $\int p_\Delta(\boldsymbol{y}_\Delta, s|\boldsymbol{x}_\Delta, t)\mathscr{G}_\lambda(\boldsymbol{y}_\Delta, \sigma_0^2)\,\mathrm{d}\boldsymbol{y}_\Delta$ in (6) and (7). This integral is illustrated schematically in figure 3. In all the regimes considered, one of the two distributions $p_\Delta(\boldsymbol{y}_\Delta, s|\boldsymbol{x}_\Delta, t)$ and $\mathscr{G}_\lambda(\boldsymbol{y}_\Delta, \sigma_0^2)$ is much wider than the other, which allows various asymptotic forms of the integral to be obtained (details are given in Appendix B). Also, when the two distributions fail to overlap significantly we know that the integral must be very small.

Figures 4, 5 and 6 show the results for the homogeneous random sources, the linear sources, and the area, line and point sources respectively. In each region of each of the figures the value given refers to the asymptotic situation well inside the region, with the exception of the results immediately to the right of $\Delta = 0$ or immediately above $\tau = 0$ which are valid right down to $\Delta = 0$ and $\tau = 0$. In figures 4 and 6 the cases below the left-to-right line through the figure are those with $d \ll \sigma_0$, i.e. p_Δ much narrower than $\mathscr{G}_\lambda(\boldsymbol{y}_\Delta, \sigma_0^2)$, while those above the line are those with $\sigma_0 \ll d$, i.e. $\mathscr{G}_\lambda(\boldsymbol{y}_\Delta, \sigma_0^2)$ much narrower than p_Δ. Note that although the figures are laid out as if $\sigma_0 \ll L$, this assumption is not necessary. As σ_0 increases towards and then exceeds L, all that happens is that some of the regions become irrelevant and some of the labels on the Δ-axis which are not associated with region boundaries need to be moved to a different point on the axis (e.g. $\Delta \simeq \sigma_0$ in figure 4 needs to be moved to after $\Delta \simeq L$).

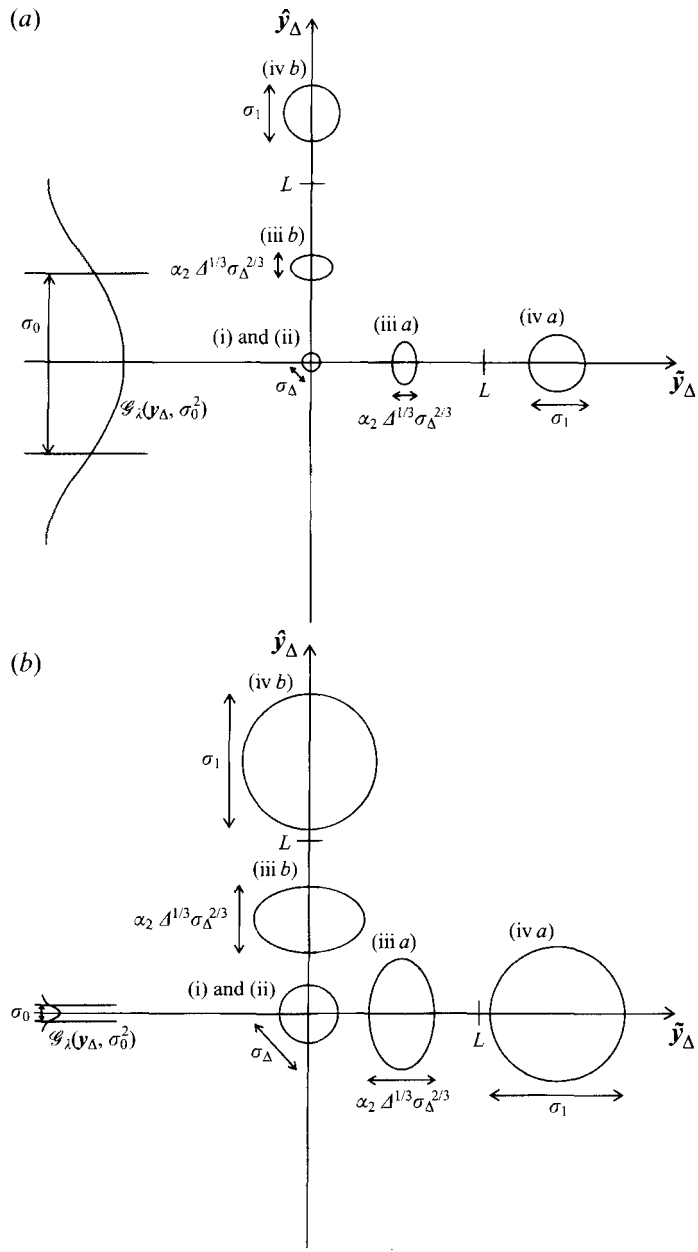

FIGURE 3. Schematic illustration of the integral $\int p_\Delta(\boldsymbol{y}_\Delta, s|\boldsymbol{x}_\Delta, t)\mathscr{G}_\lambda(\boldsymbol{y}_\Delta, \sigma_0^2)\,\mathrm{d}\boldsymbol{y}_\Delta$. The cases $d \ll \sigma_0$ and $\sigma_0 \ll d$ are shown in (*a*) and (*b*) respectively. Note that σ_0 could be greater or less than L in (*a*). The extent of the distribution $p_\Delta(\boldsymbol{y}_\Delta, s|\boldsymbol{x}_\Delta, t)$ (i.e. the region where $p_\Delta(\boldsymbol{y}_\Delta, s|\boldsymbol{x}_\Delta, t)$ is significantly non-zero) is shown for various values of $\boldsymbol{x}_\Delta$: (i) and (ii) denote the cases $\Delta = 0$ and $0 < \Delta \ll \sigma_\Delta$, (iii*a*) and (iii*b*) denote $\sigma_\Delta \ll \Delta \ll L$ with $\hat{\boldsymbol{x}}_\Delta = 0$ and $\tilde{\boldsymbol{x}}_\Delta = 0$ respectively, and (iv*a*) and (iv*b*) denote $L \ll \Delta$ with $\hat{\boldsymbol{x}}_\Delta = 0$ and $\tilde{\boldsymbol{x}}_\Delta = 0$ respectively. $\hat{\boldsymbol{x}}_\Delta = 0$ implies $\boldsymbol{x}_\Delta$ lies in the along-source direction while $\tilde{\boldsymbol{x}}_\Delta = 0$ implies $\boldsymbol{x}_\Delta$ lies in the across-source direction. Using the figure, one can see the extent to which the distributions $p_\Delta(\boldsymbol{y}_\Delta, s|\boldsymbol{x}_\Delta, t)$ and $\mathscr{G}_\lambda(\boldsymbol{y}_\Delta, \sigma_0^2)$ overlap.

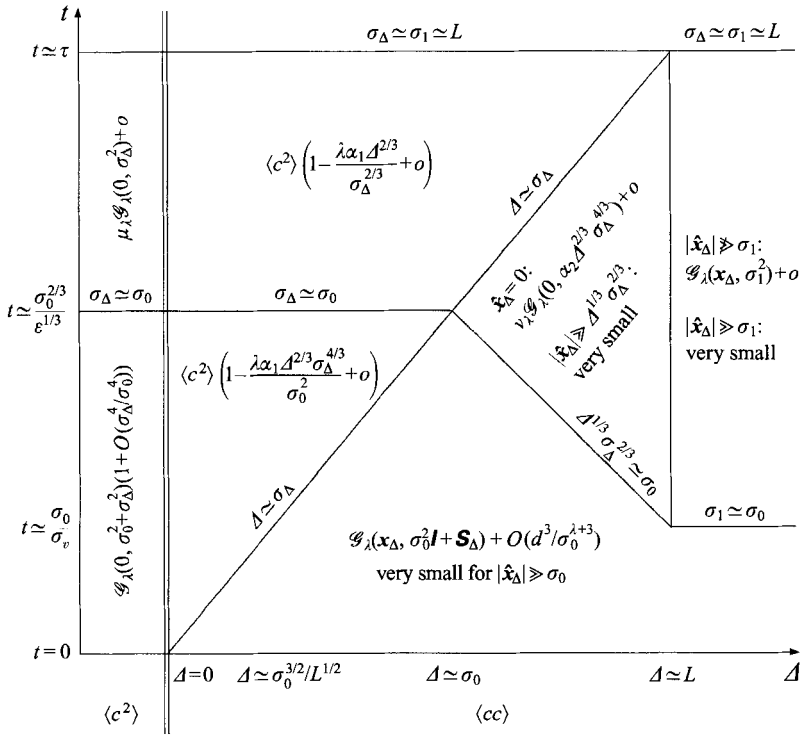

FIGURE 4. Second-order moments for homogeneous random sources. For simplicity we have taken the source time s to be zero.

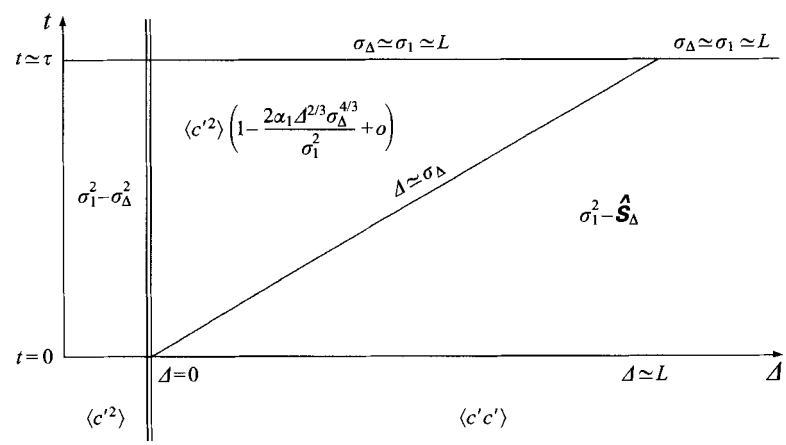

FIGURE 5. Second-order moments for linear sources. For simplicity we have taken the source time s to be zero.

For the area, line and point sources the results given (in figure 6 and below) are in general valid only for $|\hat{x}| \not\gg \max(\sigma_0, \sigma_1)$, i.e. for points not in the extreme tails of the mean plume. In the extreme tails the analysis implies of course that the quantities are very small.

There are a number of simplifications and approximations which can be made to the results in figures 4 to 6 and which make the behaviour of the second-order

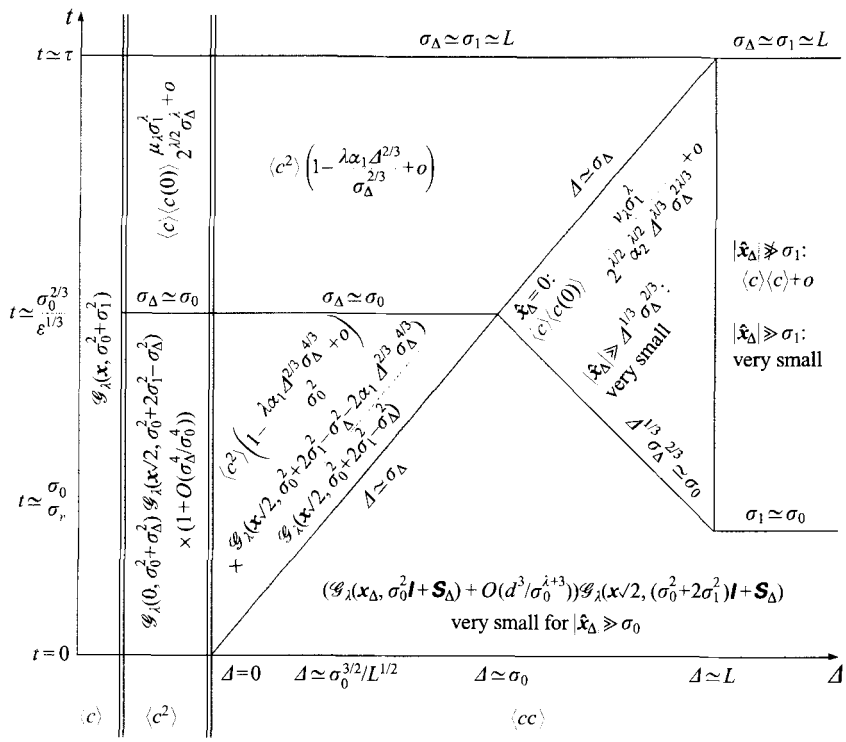

FIGURE 6. Second-order moments for area, line and point sources. For simplicity we have taken the source time s to be zero.

moments clearer. Note these simplifications and approximations do not involve any new assumptions – they are exact results in the same sense that $e^x = 1 + O(x)$ as $x \to 0$ is exact. Some of these simplifications are valid only for $|\hat{\boldsymbol{x}}_\Delta| \not\gg \max(\sigma_0, d)$, i.e. for situations where it is possible for a pair of particles with separation of order $\boldsymbol{x}_\Delta$ at the measurement time t to both pass through the source (when followed backwards to time s) without the separation at time s lying in the extreme tail of the separation p.d.f. The cases where the restriction $|\hat{\boldsymbol{x}}_\Delta| \not\gg \max(\sigma_0, d)$ is required are noted below. In the simplifications and approximations we repeatedly use a number of approximations to Gaussian distributions, namely

$$\mathscr{G}_\lambda(\boldsymbol{x}, \sigma^2\boldsymbol{I} + \boldsymbol{S}) = \mathscr{G}_\lambda(\boldsymbol{x}, \sigma^2)\left(1 - \frac{\mathrm{tr}\hat{\boldsymbol{S}}}{2\sigma^2} + \frac{\hat{\boldsymbol{x}}^T\hat{\boldsymbol{S}}\hat{\boldsymbol{x}}}{2\sigma^4} + O\left(\frac{\|\hat{\boldsymbol{S}}\|^2}{\sigma^4}\right)\right),$$

$$\mathscr{G}_\lambda(\boldsymbol{x}, \sigma^2\boldsymbol{I} + \boldsymbol{S})\mathscr{G}_\lambda(\boldsymbol{y}, \sigma^2\boldsymbol{I} - \boldsymbol{S}) = \mathscr{G}_\lambda(\boldsymbol{x}, \sigma^2)\mathscr{G}_\lambda(\boldsymbol{y}, \sigma^2)\left(1 + \frac{\mathrm{tr}(\hat{\boldsymbol{S}}\hat{\boldsymbol{S}})}{2\sigma^4} + \frac{\hat{\boldsymbol{x}}^T\hat{\boldsymbol{S}}\hat{\boldsymbol{x}}}{2\sigma^4} - \frac{\hat{\boldsymbol{y}}^T\hat{\boldsymbol{S}}\hat{\boldsymbol{y}}}{2\sigma^4} + O\left(\frac{\|\hat{\boldsymbol{S}}\|^4}{\sigma^8} + \frac{|\hat{\boldsymbol{x}}|^2\|\hat{\boldsymbol{S}}\|^2}{\sigma^6} + \frac{|\hat{\boldsymbol{y}}|^2\|\hat{\boldsymbol{S}}\|^2}{\sigma^6}\right)\right)$$

and

$$\exp\left(-\frac{\hat{\boldsymbol{x}}^T(\sigma^2\hat{\boldsymbol{I}} + \hat{\boldsymbol{S}})^{-1}\hat{\boldsymbol{x}}}{2}\right) = \exp\left(-\frac{|\hat{\boldsymbol{x}}|^2}{2\sigma^2}\right)\left(1 + \frac{\hat{\boldsymbol{x}}^T\hat{\boldsymbol{S}}\hat{\boldsymbol{x}}}{2\sigma^4} + O\left(\frac{|\hat{\boldsymbol{x}}|^2\|\hat{\boldsymbol{S}}\|^2}{\sigma^6}\right)\right)$$

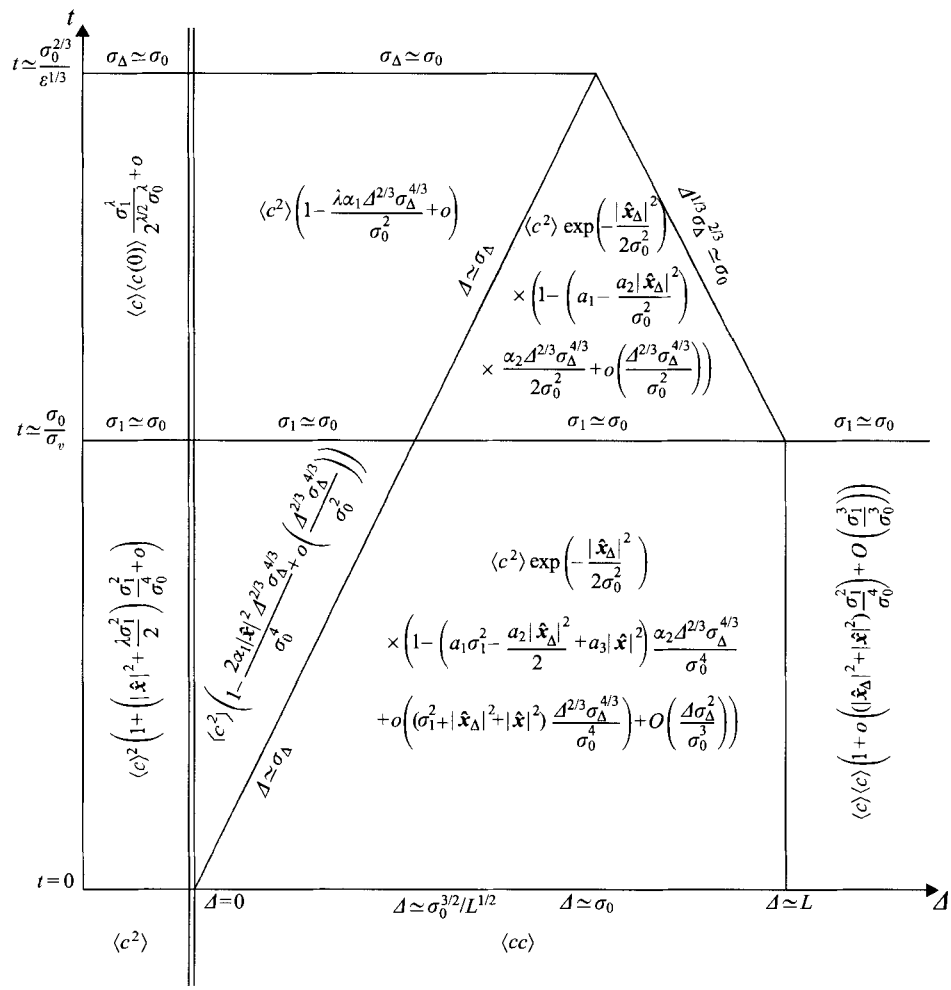

FIGURE 7. Second-order moments for area, line and point sources for $d \ll \sigma_0$, $|\hat{\mathbf{x}}_\Delta| \not\gg \sigma_0$. Results for $\sigma_1 \ll \sigma_0$ and $\sigma_0 \ll \sigma_1$ are shown separately. For simplicity we have taken the source time s to be zero.

where $\hat{\mathbf{S}}$ is symmetric and $\|\hat{\mathbf{S}}\|$ is the maximum absolute value of the eigenvalues of $\hat{\mathbf{S}}$. These approximations are valid for $\|\hat{\mathbf{S}}\| \ll \sigma^2$ and $|\hat{\mathbf{x}}|, |\hat{\mathbf{y}}| \not\gg \sigma$.

The first two simplifications are concerned with the results in the lower-right part of figures 4, 5 and 6, i.e. with the value of $\langle cc \rangle$ for $\sigma_\Delta \ll \Delta$, $d \ll \sigma_0$ (where we regard σ_0 as infinite for the linear source case). These simplifications also require $|\hat{\mathbf{x}}_\Delta| \not\gg \max(\sigma_0, d)$ $(= \sigma_0)$. The first simplification involves expressing $\langle cc \rangle$ in terms of $\langle c^2 \rangle$. For the homogeneous random sources we have

$$\langle cc \rangle = \langle c^2 \rangle \exp\left(-\frac{|\hat{\mathbf{x}}_\Delta|^2}{2\sigma_0^2}\right)\left(1 - \frac{\mathrm{tr}\hat{\mathbf{G}}}{2\sigma_0^2} + \frac{\hat{\mathbf{x}}_\Delta^T \hat{\mathbf{S}}_\Delta \hat{\mathbf{x}}_\Delta}{2\sigma_0^4} + O\left(\frac{d^3}{\sigma_0^3}\right)\right), \tag{9}$$

for the linear sources we have

$$\langle c'c' \rangle = \langle c'^2 \rangle \left(1 - \frac{\hat{\mathbf{G}}}{\sigma_1^2 - \sigma_\Delta^2}\right) \tag{10}$$

and for the area, line and point sources we have

$$\langle cc\rangle = \langle c^2\rangle \exp\left(-\frac{|\hat{\boldsymbol{x}}_\Delta|^2}{2\sigma_0^2}\right)\left(1-\frac{\mathrm{tr}\hat{\mathbf{G}}}{2\sigma_0^2}+\frac{\mathrm{tr}\hat{\mathbf{G}}}{2(\sigma_0^2+2\sigma_1^2)}+\frac{\hat{\boldsymbol{x}}_\Delta^T\hat{\mathbf{S}}_\Delta\hat{\boldsymbol{x}}_\Delta}{2\sigma_0^4}-\frac{\hat{\boldsymbol{x}}^T\hat{\mathbf{G}}\hat{\boldsymbol{x}}}{(\sigma_0^2+2\sigma_1^2)^2}+O\left(\frac{d^3}{\sigma_0^3}\right)\right). \tag{11}$$

Here $\mathbf{G}$ denotes $\mathbf{S}_\Delta - \sigma_\Delta^2\mathbf{I}$. The second simplification is concerned with making use of our knowledge of $\mathbf{S}_\Delta$ as summarized in §4. We have avoided making use of this knowledge so far in the lower-right part of figures 4, 5 and 6 because this has enabled us to obtain results valid for all $\Delta \gg \sigma_\Delta$ (and not just for $\sigma_\Delta \ll \Delta \ll L$ and $L \ll \Delta$ separately) and also because this avoids the need to derive (9), (10) and (11) separately for $\sigma_\Delta \ll \Delta \ll L$ and $L \ll \Delta$. (We could similarly have avoided using our knowledge of p_Δ for $\sigma_\Delta \ll \Delta$, $\sigma_0 \ll d$, i.e. for the upper-right parts of figures 4 and 6. However there is less to be gained by this because there is no simplification analogous to (9), (10) and (11) and because estimating aspects of p_Δ beyond those given in §4 is likely to be more difficult than doing the same for $\mathbf{S}_\Delta$.) By making use of our knowledge of $\mathbf{S}_\Delta$ we obtain the following results. For the homogeneous random sources we have

$$\langle cc\rangle = \langle c^2\rangle \exp\left(-\frac{|\hat{\boldsymbol{x}}_\Delta|^2}{2\sigma_0^2}\right)\left(1-\left(a_1-\frac{a_2|\hat{\boldsymbol{x}}_\Delta|^2}{\sigma_0^2}\right)\frac{\alpha_2\Delta^{2/3}\sigma_\Delta^{4/3}}{2\sigma_0^2}+o\left(\frac{\Delta^{2/3}\sigma_\Delta^{4/3}}{\sigma_0^2}\right)\right)$$

for $\sigma_\Delta \ll \Delta \ll L$ and

$$\langle cc\rangle = \mathscr{G}_\lambda(\boldsymbol{x}_\Delta, \sigma_0^2+\sigma_1^2)\left(1+o\left(\frac{\sigma_1^2}{\sigma_0^2}\right)\right)$$

for $L \ll \Delta$; for the linear sources we have

$$\langle c'c'\rangle = \langle c'^2\rangle\left(1-\frac{a_1\alpha_2\Delta^{2/3}\sigma_\Delta^{4/3}}{\sigma_1^2}+o\right)$$

for $\sigma_\Delta \ll \Delta \ll L$ and

$$\langle c'c'\rangle = o(\sigma_1^2)$$

for $L \ll \Delta$; and for the area, line and point sources we have

$$\begin{aligned}\langle cc\rangle = \langle c^2\rangle \exp\left(-\frac{|\hat{\boldsymbol{x}}_\Delta|^2}{2\sigma_0^2}\right)&\\ \times\left(1-\left(\frac{a_1}{2\sigma_0^2}-\frac{a_1}{2(\sigma_0^2+2\sigma_1^2)}-\frac{a_2|\hat{\boldsymbol{x}}_\Delta|^2}{2\sigma_0^4}+\frac{a_3|\hat{\boldsymbol{x}}|^2}{(\sigma_0^2+2\sigma_1^2)^2}\right)\alpha_2\Delta^{2/3}\sigma_\Delta^{4/3}\right.&\\ \left.+o\left(\left(\frac{\sigma_1^2}{\sigma_0^2\max(\sigma_0^2,\sigma_1^2)}+\frac{|\hat{\boldsymbol{x}}_\Delta|^2}{\sigma_0^4}+\frac{|\hat{\boldsymbol{x}}|^2}{\max(\sigma_0^4,\sigma_1^4)}\right)\Delta^{2/3}\sigma_\Delta^{4/3}\right)+O\left(\frac{\Delta\sigma_\Delta^2}{\sigma_0^3}\right)\right)&\end{aligned} \tag{12}$$

for $\sigma_\Delta \ll \Delta \ll L$ and

$$\langle cc\rangle = \langle c\rangle\langle c\rangle\left(1+o\left((|\hat{\boldsymbol{x}}_\Delta|^2+|\hat{\boldsymbol{x}}|^2)\frac{\sigma_1^2}{\sigma_0^4}\right)+O\left(\frac{\sigma_1^3}{\sigma_0^3}\right)\right) \tag{13}$$

for $L \ll \Delta$. In these equations a_1, a_2 and a_3 are geometric factors defined by

$$a_1 = \frac{4}{3}\lambda - \frac{1}{3}\frac{|\hat{\boldsymbol{x}}_\Delta|^2}{\Delta^2}, \quad a_2 = \frac{4}{3}-\frac{1}{3}\frac{|\hat{\boldsymbol{x}}_\Delta|^2}{\Delta^2}, \quad a_3 = \frac{4}{3}-\frac{1}{3}\frac{(\hat{\boldsymbol{x}}_\Delta.\hat{\boldsymbol{x}})^2}{\Delta^2|\hat{\boldsymbol{x}}|^2}.$$

The third simplification concerns the value of $\langle cc\rangle$ for $0 < \Delta \ll \sigma_\Delta$, $d \ll \sigma_0$ in the case of

the area, line and point sources. Here we can expand the Gaussian in the numerator to get

$$\langle cc\rangle = \langle c^2\rangle\left(1-\left(\frac{\lambda}{\sigma_0^2}-\frac{\lambda}{\sigma_0^2+2\sigma_1^2}+\frac{2|\hat{\boldsymbol{x}}|^2}{(\sigma_0^2+2\sigma_1^2)^2}\right)\alpha_1\Delta^{2/3}\sigma_\Delta^{4/3}+o\left(\frac{\Delta^{2/3}\sigma_\Delta^{4/3}}{\sigma_0^2}\right)\right).$$

The final simplification is concerned with the area, line and point sources for $d \ll \sigma_0$, $|\hat{\boldsymbol{x}}_\Delta| \not\gg \sigma_0$. For these cases the results simplify considerably if we consider the cases $\sigma_1 \ll \sigma_0$ and $\sigma_0 \ll \sigma_1$ separately. The results are shown in figure 7.

There are a number of areas where more complete results can be obtained. For the homogeneous random sources and the area, line and point sources we can obtain results which are valid in more than one region of figures 4 and 6. In particular $\langle cc\rangle$ is very small throughout the region $|\hat{\boldsymbol{x}}_\Delta| \gg \max(\sigma_0, d)$. Also $\langle cc\rangle$ equals $\mathscr{G}_\lambda(\boldsymbol{x}_\Delta, \sigma_0^2+\sigma_1^2)+o$ for the homogeneous random sources and $\langle c\rangle\langle c\rangle+o$ for the area, line and point sources throughout the region $L \ll \Delta$, $|\hat{\boldsymbol{x}}_\Delta| \not\gg \max(\sigma_0, d)$ ($\simeq \max(\sigma_0, \sigma_1)$). In addition we have not given the greatest accuracy possible for $\langle c^2\rangle$ in figure 7 – the values have been simplified in order to try and make the qualitative behaviour as clear as possible.

Before discussing the results given above, we will consider their accuracy. If the material in §§3 and 4 is correct, then the results above are also correct. Of course the results presented in §3 are not exact (see discussion in that section) and the classical picture in §4 is almost certainly incorrect in detail (e.g. due to intermittency effects). However, with the possible exception of the effect of errors in the Sawford approximation which is used for the area, line and point sources, the results are robust to small errors in §§3 and 4. Hence, provided the problems with the Sawford approximation are unimportant, the results should be good approximations. In order to see how sensitive the results are to the Sawford approximation, we will investigate how much the results would be altered if the Sawford approximation were replaced by a symmetrized form as discussed in §3. It turns out that this could alter some of the above results. Firstly the value of $\langle c^2\rangle$ for $\sigma_\Delta \ll \sigma_0$ in figure 6 could be altered by a factor of $1+O(\sigma_\Delta^2/\max(\sigma_0^2, \sigma_1^2))$. This has a small and not very important effect on the results (and does not affect the simplified results in figure 7) except for $\sigma_1 \ll \sigma_0$ where it could have a leading-order effect on $\langle c^2\rangle - \langle c\rangle^2$ near $\hat{\boldsymbol{x}} = 0$. Secondly $\langle cc\rangle$ could be altered for $0 < \Delta \ll \sigma_\Delta$, $d \ll \sigma_0$ by a factor of $1+O(\Delta^{2/3}\sigma_\Delta^{4/3}/\max(\sigma_0^2, \sigma_1^2))$. For $\sigma_0 \ll \sigma_1$ this would not alter the results, but elsewhere this could have a leading-order effect on $\langle c^2\rangle - \langle cc\rangle$. Finally $\langle cc\rangle$ could be altered very slightly for $\sigma_\Delta \ll \Delta$, $d \ll \sigma_0$. However, because $\boldsymbol{S}_\Delta$ is only known to leading order, this has no effect once our knowledge of $\boldsymbol{S}_\Delta$ has been used (equations (12) and (13) and figure 7). The more serious of these problems are for $0 \leqslant \Delta \ll \sigma_\Delta$, $\sigma_1 \ll \sigma_0$ and it is only then that the simplified results in figure 7 are affected. Despite the above, we should not take too pessimistic a view of the accuracy of the results – as noted in §3, simply symmetrizing Sawford's p_2 may make the approximation rather less consistent.

In order to assess whether these problems are significant, we can consider a number of alternative ways of deriving the second-order moments of c for the cases where our doubts about the validity of the results are most serious, namely the area, line and point source cases for $0 \leqslant \Delta \ll \sigma_\Delta$, $\sigma_1 \ll \sigma_0$. Throughout this paragraph we restrict attention to these cases. Note that the arguments above gave us no reason to doubt that $\langle c^2\rangle$ and $\langle cc\rangle$ are not correct to leading order – our interest here is in the differences $\langle c^2\rangle - \langle c\rangle^2$ and $\langle c^2\rangle - \langle cc\rangle$. Firstly we note that, for $|\hat{\boldsymbol{x}}| \gg \sigma_1$, the change in the gradient of the source over the region where p_2 is significantly non-zero is small compared to the gradient itself. Hence it should be possible to approximate the source

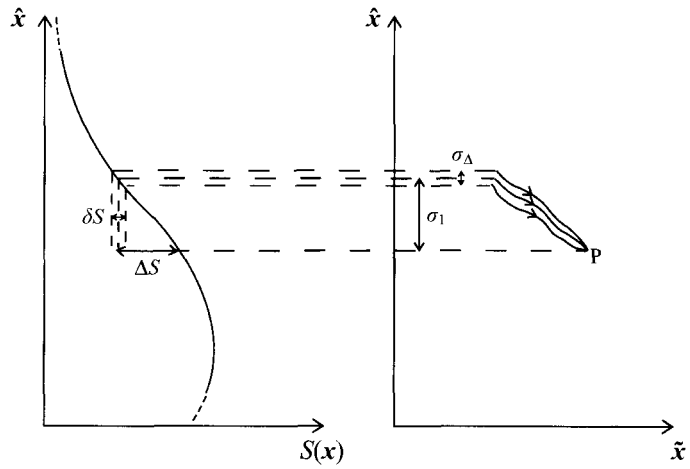

FIGURE 8. Schematic illustration of the trajectories of particles arriving at a point P in one realization of the flow for $\sigma_1 \ll \sigma_0$.

by a linear source, although it is hard to estimate the error in doing this. Calculations done with this approximation support the results in figure 7 for $|\hat{\boldsymbol{x}}| \gg \sigma_1$. For smaller $|\hat{\boldsymbol{x}}|$, figure 7 gives a quantitative prediction for $\langle c^2\rangle - \langle c\rangle^2$ but only gives an order of magnitude bound on $\langle c^2\rangle - \langle cc\rangle$. The trend in the results obtained with the linear source approximation as $\hat{\boldsymbol{x}} \to 0$ cannot of course support the quantitative prediction for $\langle c^2\rangle - \langle c\rangle^2$ but lends support to the bound on $\langle c^2\rangle - \langle cc\rangle$ if we assume, as seems plausible, that $\langle c^2\rangle - \langle cc\rangle$ varies monotonically with $|\hat{\boldsymbol{x}}|$ as $\hat{\boldsymbol{x}}$ decreases through σ_1 to zero. Secondly, for the cases being considered, p_2 is narrower than the source in all directions and so we can calculate $\langle c^2\rangle$ by applying the first lemma in Appendix B directly without needing the Sawford approximation. This calculation gives

$$\langle c^2\rangle = \langle c\rangle^2 \left(1 + \left(|\hat{\boldsymbol{x}}|^2 + \frac{\lambda\sigma_1^2}{2}\right)\frac{\sigma_1^2}{\sigma_0^4} + O\left(\frac{\sigma_1^4}{\sigma_0^4}\right)\right).$$

This supports the value in figure 7 for $|\hat{\boldsymbol{x}}| \gg \sigma_1$, but only gives an order of magnitude bound on $\langle c^2\rangle - \langle c\rangle^2$ near $\hat{\boldsymbol{x}} = 0$. However the error term in the lemma is due to the non-Gaussianity of p_2 and this non-Gaussianity is associated with the scale σ_Δ not σ_1. Hence the lemma may be giving a pessimistic error estimate and the result in figure 7 may be correct down to $\hat{\boldsymbol{x}} = 0$. Finally it seems probable that at such short times it is a reasonable approximation to calculate $\langle c^2\rangle - \langle c\rangle^2$ by representing the dispersion as simply a bulk displacement of the source profile without change of shape. This can be justified by considering the particles arriving at a point P in one realization of the flow (see figure 8). The variation in the starting points of the particle trajectories is small (of order σ_Δ) compared to the bulk displacement (of order σ_1) and so, because $\sigma_\Delta \ll \sigma_0$, the variation δS in S between these starting positions can be neglected compared to the difference ΔS between S at the starting position and at P. Hence the change in concentration between time s and time t is dominated by bulk displacement. Calculations with the bulk displacement assumption (similar to those in Gifford's 1959 fluctuating plume model) support the value given in figure 7. From these arguments we conclude that the results in question are probably correct, at least in the simplified forms given in figure 7.

6. Discussion

In this section we will discuss the results in §5 and try to give some simple physical pictures of what is happening in each regime. Several of the results are well-established (such as the inertial–convective subrange behaviour for $0 < \Delta \ll \sigma_\Delta$) but there are also a number of new and interesting results (such as the 'inertial–meander' subrange discussed below).

6.1. *One-point moments*

Consider first the one-point moments. For the homogeneous random sources, $\langle c^2 \rangle$ has two regimes with the transition occurring when $\sigma_\Delta \simeq \sigma_0$, i.e. when it is possible to bring together particles which come from points for which, at the source time, the concentrations differ significantly. When this is possible we expect mixing to occur with $\langle c^2 \rangle$ decreasing and ε_c becoming significant. When $\sigma_\Delta \ll \sigma_0$, i.e. in the first regime, the particles arriving at a given point must, in any one realization of the flow, have come from points for which, at the source time, the concentrations were highly correlated. Hence $\langle c^2 \rangle$ is approximately equal to its initial value. When $\sigma_0 \ll \sigma_\Delta$, i.e. in the second regime, the source $\langle S(\boldsymbol{y}_1) S(\boldsymbol{y}_2) \rangle$ can be approximated by a delta-function concentrated at $\hat{\boldsymbol{y}}_\Delta = 0$ and so $\langle c^2 \rangle$ varies like $1/\sigma_\Delta^\lambda$, with the coefficient depending on the shape of p_Δ.

For the linear source the situation is simpler with only one regime. This is essentially because there is no length-scale associated with the source. The particles in the ensemble of realizations which arrive at a given point must have come from points for which the concentrations, at the source time, have a (root-mean-square) variability equal to σ_1. Also, because $\sigma_\Delta \ll \sigma_1$, the particles *in any one realization* which arrive at the point must have come from points for which the variability is much less. Hence, to leading order, mixing can be neglected, c' is proportional to the displacement of a particle, and $\langle c'^2 \rangle = \sigma_1^2$.

Finally we consider the area, line and point sources. Here we have three regimes illustrated in figure 9. The two transitions occur when $\sigma_1 \simeq \sigma_0$, i.e. when the scale of the meandering becomes comparable to the source size, and when $\sigma_\Delta \simeq \sigma_0$, i.e. when it is possible to bring together particles which come from points for which the concentrations at the source time are significantly different. As for the homogeneous random sources we expect mixing to occur with $\int \langle c^2 \rangle \, \mathrm{d}\hat{\boldsymbol{x}}$ decreasing and ε_c becoming significant when σ_Δ becomes comparable to σ_0. Note also that, considering particles travelling forward in time from the source, the change in separation for particles with initial separation of order σ_0 is of order σ_Δ for $\sigma_0 \ll \sigma_\Delta$, of order $\sigma_0^{1/3} \sigma_\Delta^{2/3}$ for $\sigma_\Delta \ll \sigma_0 \ll L$ and of order σ_1 for $L \ll \sigma_0$. Hence the time when $\sigma_\Delta \simeq \sigma_0$ is also the time at which this change in separation becomes comparable to σ_0 and the cloud of contaminant begins to distort and break up; for $\sigma_\Delta \ll \sigma_0$ the cloud remains coherent in the sense that the concentration profile in the cross-source direction is, at any given along-source position, simply a displacement of the source profile. The root-mean-square instantaneous plume width in the cross-source direction (more precisely the root-mean-square width of the 'mean instantaneous plume', the mean instantaneous plume being defined as the ensemble mean of the cross-source concentration profiles with the centres of mass of the profiles aligned before averaging) is of order the larger of σ_0 and the change in separation for particles with initial separation of order σ_0, i.e. it is of order $\max(\sigma_0, \sigma_\Delta)$. When $\sigma_1 \ll \sigma_0$, i.e. in the first regime, the width of the ensemble mean concentration field and the root-mean-square instantaneous plume width are equal to leading order and so the amount of plume meander is small

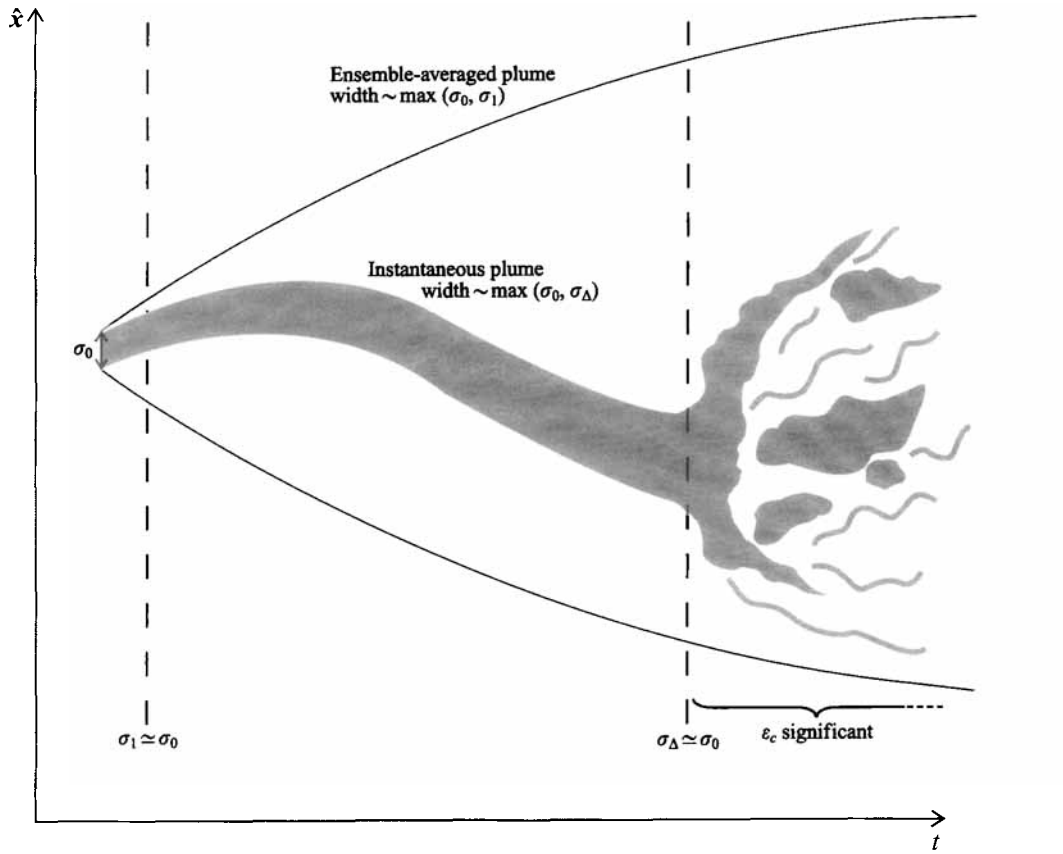

FIGURE 9. Schematic illustration of the dispersion from area, line and point sources.

compared to the plume width. However, when $\sigma_0 \ll \sigma_1$, i.e. in the second and third regimes, the root-mean-square instantaneous plume width is much less than the width of the ensemble mean concentration field and so the plume is narrow compared to the distance over which it meanders. In the first two regimes, $\sigma_1 \ll \sigma_0$ and $\sigma_\Delta \ll \sigma_0 \ll \sigma_1$, $\langle c^2 \rangle$ evolves as one would expect from a coherent meandering Gaussian cloud (Gifford 1959). In the third regime, $\sigma_0 \ll \sigma_\Delta$, the source $S(\boldsymbol{y})$ can be approximated by a delta-function concentrated at $\hat{\boldsymbol{y}} = 0$ leading to a root-mean-square instantaneous plume width equal to $\sigma_\Delta(t|s)$ (Batchelor 1952). Here Gifford's fluctuating ('meandering' would be a better word – there are no 'in-plume' fluctuations) plume model provides some insight into the scaling of the result although the actual $\langle c^2 \rangle$ is greater by a factor $\mu_\lambda(\sigma_\Delta(t|s)/\sigma_\Delta(s|t))^\lambda$ (this factor is in fact the equivalent of μ_λ for the forward dispersion form of p_Δ) which represents the in-plume fluctuations and any non-Gaussianity of the mean instantaneous plume. As expected from random walk simulations (Thomson 1990), σ_c $(= \langle c'^2 \rangle^{1/2})$ peaks away from the centreline (i.e. away from $\hat{\boldsymbol{x}} = 0$) initially, with the peak moving to the centreline when $\sigma_1 \simeq \sigma_0$. The overall peak in σ_c (in time as well as space) occurs when $\sigma_1 \simeq \sigma_0$. In contrast $\sigma_c/\langle c \rangle$ always has a minimum on the centreline and the peak centreline value of $\sigma_c/\langle c \rangle$ occurs when $\sigma_\Delta \simeq \sigma_0$.

6.2. *Two-point moments*

We will now consider the two-point moments. For $0 < \Delta \ll \sigma_\Delta$ we have the standard inertial–convective subrange scaling $\alpha - \beta \Delta^{2/3}$. These results arise from the 'time-

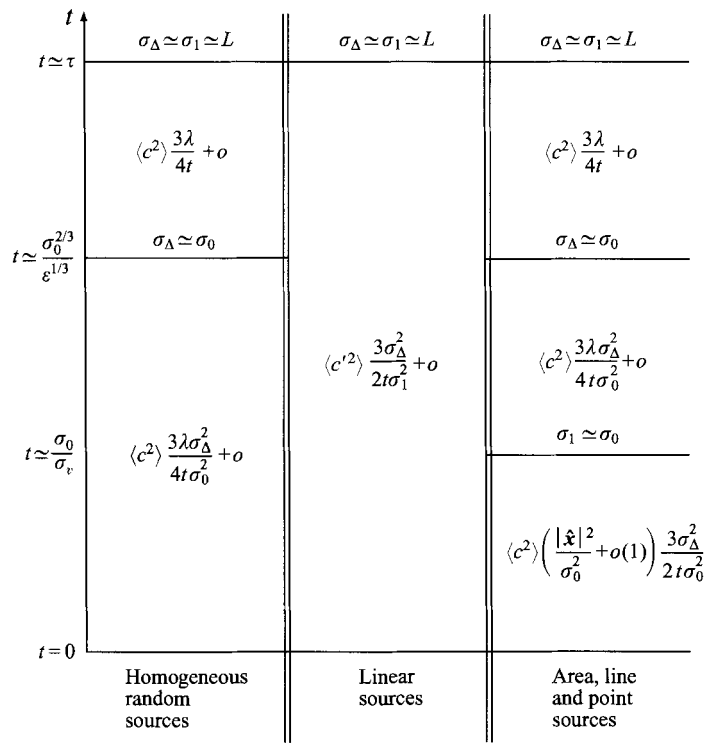

FIGURE 10. Values of ε_c for the various source types. For simplicity we have taken the source time s to be zero.

advancement' of p_Δ described in case (ii) of §4 and suggest that the inertial subrange can in general be viewed as a consequence of the time advancement. It is possible to infer the implied value of ε_c for the inertial–convective subrange. The results are shown in figure 10. It is also possible as a check to derive ε_c from $\langle c^2 \rangle$ for the homogeneous random sources and from $\langle c'^2 \rangle$ for the linear sources and to derive $\int \varepsilon_c \, \mathrm{d}\hat{\boldsymbol{x}}$ for the area, line and point sources from $\int \langle c^2 \rangle \mathrm{d}\hat{\boldsymbol{x}}$. While this consistency is a useful check, it is easy to show that for the types of sources considered here such consistency must follow from the time-advancement assumption of Batchelor (1952). This is true even for non-Gaussian source shapes. For example, for the homogeneous random sources we have

$$\langle c^2 \rangle = \int p_\Delta(\boldsymbol{y}_\Delta, s|0, t) \langle S(\boldsymbol{y}_1) S(\boldsymbol{y}_2) \rangle \, \mathrm{d}\boldsymbol{y}_1 \, \mathrm{d}\boldsymbol{y}_2$$

and

$$2\varepsilon_c = -\frac{\mathrm{d}\langle c^2 \rangle}{\mathrm{d}t} = \int \frac{\mathrm{d}}{\mathrm{d}t} p_\Delta(\boldsymbol{y}_\Delta, s|0, t) \langle S(\boldsymbol{y}_1) S(\boldsymbol{y}_2) \rangle \, \mathrm{d}\boldsymbol{y}_1 \, \mathrm{d}\boldsymbol{y}_2$$

which leads to

$$\begin{aligned} \langle c(\boldsymbol{x}_1, t) c(\boldsymbol{x}_2, t) \rangle &= \int p_\Delta(\boldsymbol{y}_\Delta, s|\boldsymbol{x}_\Delta, t) \langle S(\boldsymbol{y}_1) S(\boldsymbol{y}_2) \rangle \, \mathrm{d}\boldsymbol{y}_1 \, \mathrm{d}\boldsymbol{y}_2 \\ &\simeq \int p_\Delta(\boldsymbol{y}_\Delta, s|0, t + \frac{C_\theta \Delta^{2/3}}{2^{5/3} \varepsilon^{1/3}}) \langle S(\boldsymbol{y}_1) S(\boldsymbol{y}_2) \rangle \, \mathrm{d}\boldsymbol{y}_1 \, \mathrm{d}\boldsymbol{y}_2 \end{aligned}$$

$$\simeq \langle c^2\rangle + \frac{C_\theta \Delta^{2/3}}{2^{5/3}\varepsilon^{1/3}}\frac{\mathrm{d}\langle c^2\rangle}{\mathrm{d}t}$$

$$\simeq \langle c^2\rangle - \frac{C_\theta}{2}\varepsilon_c\varepsilon^{-1/3}(\Delta\sqrt{2})^{2/3}.$$

Note that, for the area, line and point sources, our analysis is not sufficient to enable us to estimate $\langle c^2\rangle - \langle cc\rangle$ for $0 < \Delta \ll \sigma_\Delta$, $\sigma_1 \ll \sigma_0$, $|\hat{\boldsymbol{x}}| \ll \sigma_0$. As a result we cannot obtain ε_c for $\sigma_1 \ll \sigma_0$, $|\hat{\boldsymbol{x}}| \ll \sigma_0$. It does not appear possible to avoid this problem with the approach adopted here.

At larger separations than σ_Δ a more diverse range of behaviour is observed. Some of the results appear quite complex and it is perhaps easiest to understand the results by considering separately the behaviour for separations in the across-source direction ($\tilde{\boldsymbol{x}}_\Delta = 0$) and in the along-source direction ($\hat{\boldsymbol{x}}_\Delta = 0$). Note that the along-source direction only makes sense if $\lambda = 1$ or 2; if $\lambda = 3$ there is no along-source direction. Our main aim here is to understand the length scale on which $\langle cc\rangle$ decays. Consider first the linear sources. Here c' is proportional to the displacement of a particle and particle displacements are correlated for Δ of order L or smaller. Hence $\langle c'c'\rangle$ decays on the scale L. It is interesting to note that $\langle c'c'\rangle$ retains the inertial-subrange type of scaling for $\sigma_\Delta \ll \Delta \ll L$, although $\langle c'c'\rangle$ is no longer isotropic with the behaviour in the along- and across-source directions being quantitatively different. We will now consider the homogeneous random sources and the area, line and point sources. It is convenient to consider these together since there are many similarities between the two cases and to describe them separately would involve much repetition. However since our main interest is in the area, line and point sources, the discussion will focus on this case with any differences which apply to the homogeneous random sources being given in square brackets []. Consider particle pairs with positions $\boldsymbol{x}_1$ and $\boldsymbol{x}_2$ at time t. To understand the behaviour for separations $\boldsymbol{x}_1 - \boldsymbol{x}_2$ in the cross-source direction, consider the fraction of particle pairs for which both particles pass through the source [for which the source concentrations at the particle positions at time s are significantly correlated]. $\langle cc\rangle$ decays as this fraction decreases relative to the fraction for pairs with zero separation at time t. This happens when Δ reaches $\max(\sigma_0, \sigma_\Delta)$ and hence $\langle cc\rangle$ decays on the scale $\max(\sigma_0, \sigma_\Delta)$. For along-source separations the situations is more complex. Firstly $\langle cc\rangle$ does not decay to zero for large Δ but to $\langle c\rangle^2$ $[\mathscr{G}_\lambda(\boldsymbol{x}_\Delta, \sigma_0^2 + \sigma_1^2)]$. We expect $\langle cc\rangle \simeq \langle c\rangle^2$ $[\langle cc\rangle \simeq \mathscr{G}_\lambda(\boldsymbol{x}_\Delta, \sigma_0^2 + \sigma_1^2)]$ for $\Delta \gg L$ – in this regime we can assume the particles move independently. Perhaps the easiest way to discuss the results is to consider the length scale on which $\langle cc\rangle$ decreases to a significant fraction of $\langle c^2\rangle$, say to $\langle c^2\rangle/2$. For times with $\sigma_1 \ll \sigma_0$ this never happens as $\langle c\rangle^2$ $[\mathscr{G}_\lambda(\boldsymbol{x}_\Delta, \sigma_0^2 + \sigma_1^2)]$ itself is close in value to $\langle c^2\rangle$; instead $\langle cc\rangle$ decays to $\langle c\rangle^2$ $[\mathscr{G}_\lambda(\boldsymbol{x}_\Delta, \sigma_0^2 + \sigma_1^2)]$ on the length scale L. For times with $\sigma_\Delta \ll \sigma_0 \ll \sigma_1$, particles which are coincident at time t come from locations where the source concentrations are almost identical. When Δ is large enough so that $d \simeq \sigma_0$ (i.e. $\Delta^{1/3}\sigma_\Delta^{2/3} \simeq \sigma_0$) the particles are likely to come from places with significantly different source concentrations – hence $\langle cc\rangle$ decreases significantly on the scale $\sigma_0^3/\sigma_\Delta^2$. For times with $\sigma_0 \ll \sigma_\Delta$, even particles which are coincident at time t are likely to come from places with different source concentrations. The fraction of particle pairs for which both particles pass through the source [the particles come from points with significantly correlated source concentrations] decreases significantly from its value for $\Delta = 0$ when $d - \sigma_\Delta \simeq \sigma_\Delta$, i.e. when $\Delta \simeq \sigma_\Delta$. Hence $\langle cc\rangle$ decreases on the scale σ_Δ.

For $\sigma_0 \ll \sigma_1$ we have seen that $\langle cc\rangle$ decays significantly before Δ reaches L. However as Δ increases beyond the point where $\langle cc\rangle$ has decayed significantly, $\langle cc\rangle$ does not

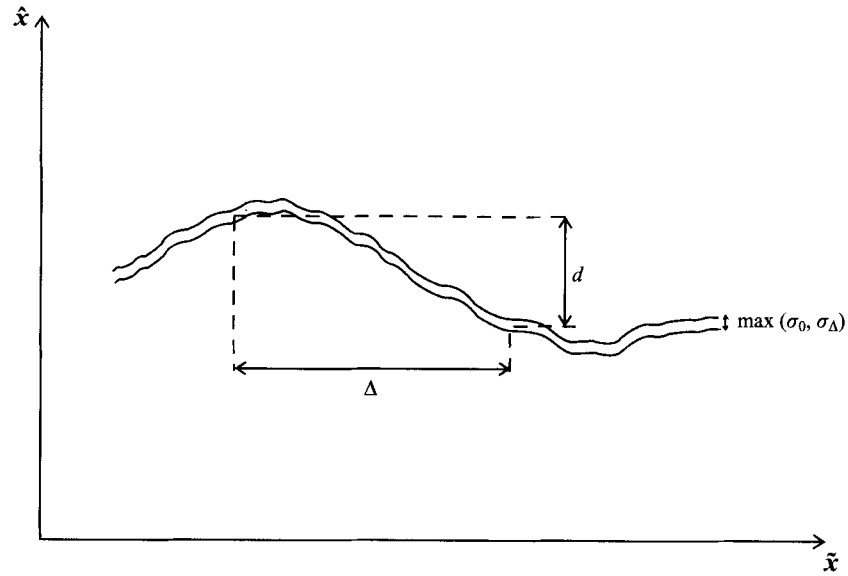

FIGURE 11. Illustration of the processes involved in the inertial–meander subrange.

rapidly converge to $\langle c\rangle^2$ $[\mathscr{G}_\lambda(\boldsymbol{x}_\Delta, \sigma_0^2 + \sigma_1^2)]$ but decays slowly and only approaches $\langle c\rangle^2$ $[\mathscr{G}_\lambda(\boldsymbol{x}_\Delta, \sigma_0^2 + \sigma_1^2)]$ when Δ is of order L. This behaviour can be seen in figures 4 and 6 for $\sigma_\Delta \ll \Delta \ll L$, $\sigma_0 \ll d$. Here the along-source correlation function has a long tail proportional to $\Delta^{-\lambda/3}$. This long tail results in an integral scale which is much larger than the scale on which $\langle cc\rangle$ decays to $\langle c^2\rangle/2$. We will discuss this behaviour in more detail only for the area, line and point sources, although an analogous discussion is possible for the homogeneous random sources. The regime $\sigma_\Delta \ll \Delta \ll L$, $\sigma_0 \ll d$ corresponds to values of Δ which (i) are much smaller than L, (ii) are much larger than the instantaneous plume, and (iii) are large enough so that d is much larger than the instantaneous plume. Condition (i) implies that eddies of scale Δ lie in the inertial subrange. Condition (ii) implies that the eddies of scale Δ move the plume coherently while (iii) implies that such eddies move the plume laterally by a distance much greater than the plume width – taken together these imply that the effect of such eddies on the plume is to cause meandering. Hence we will call this regime the inertial–meander subrange (see figure 11). This behaviour corresponds to the spectrum of c having a lot of low-frequency energy and varying with wavenumber k as $k^{(\lambda/3-1)}$. For the instantaneous line source (or continuous point source) this is $k^{-1/3}$ while for the instantaneous area source (or continuous cross-wind line source) this is $k^{-2/3}$. This subrange has in fact been observed for a continuous point source at short range in the atmosphere (Mylne, Davidson & Thomson 1996).

7. Summary

It has been shown how it is possible to use classical ideas to develop a picture of the phenomenology of the evolution of the two-point second-order moments of concentration for a variety of source configurations in isotropic turbulence. Of particular interest is the existence of an 'inertial–meander' subrange for instantaneous area and line sources (and continuous cross-wind line and point sources in a strong uniform mean flow). It seems likely that the ideas presented here could be extended to

a wider range of conditions, for example to non-isotropic (but homogeneous) flows, to travel times and length scales beyond the scales associated with the small-scale end of the inertial–convective subrange (although there is not much new to learn here), to travel times greater than τ, and to a wider range of source types (including the case of two or more sources).

Appendix A. O and o notation

Precise definitions of O and o are not entirely straightforward because we are usually considering several asymptotic limits simultaneously. For example all the results require $t-s$ to be much less than τ and much greater than the time scale associated with the small-scale end of the inertial–convective subrange. In most cases there are also further requirements.

For a result which is stated to be valid for $a_i \ll b_i$, $i = 1,\ldots,n$, $O(a)$ indicates a quantity which is bounded in absolute value by $K|a|$ for some K when the a_i/b_i are sufficiently small. Similarly $o(a)$ indicates a quantity which, for any given quantity δ, is bounded in absolute value by $\delta|a|$ when the a_i/b_i are sufficiently small. We require K and the smallness required for a_i/b_i to be independent of all quantities on which the term written as $O(a)$ or $o(a)$ depends. These definitions are of course essentially the usual ones, except that we have made it explicit that the constraints on the size of the terms $O(a)$ and $o(a)$ are uniform across all quantities. For example, for $\sigma' \ll \sigma$ we have

$$\frac{x^2}{2(\sigma^2+\sigma'^2)} = \frac{x^2}{2\sigma^2} + O\left(\frac{x^2\sigma'^2}{\sigma^4}\right)$$

and we can take K to be independent of x as well as of σ and σ'.

Some results are stated to be valid provided $a_i \ll b_i$, $i = 1,\ldots,n$ and $c_i \not\gg d_i$, $i = 1,\ldots,n'$. In such cases $O(a)$ and $o(a)$ have similar meanings, except that we do not require K and the smallness required for a_i/b_i to be completely independent of all quantities. Instead we only require that, for any choice of $K_i > 0$ $(i = 1,\ldots,n')$, K and the smallness required for a_i/b_i can be chosen to be independent of all quantities on which the term written as $O(a)$ or $o(a)$ depends as these quantities vary subject to the constraints $|c_i/d_i| \leqslant K_i$. For example, provided $\sigma' \ll \sigma$ and $x \not\gg \sigma$ we have

$$\exp\left(-\frac{x^2}{2(\sigma^2+\sigma'^2)}\right) = \exp\left(-\frac{x^2}{2\sigma^2}\right)\left(1+O\left(\frac{x^2\sigma'^2}{\sigma^4}\right)\right),$$

but note that as x/σ increases, we need to increase K or require σ'/σ to be smaller.

Appendix B. Evaluation of the integral in equations (6) and (7)

Here we present without proof four lemmas which are useful in obtaining the required results and show how these are used to evaluate the integral in equations (6) and (7). These lemmas all concern the evaluation of integrals of the form $\int p(\boldsymbol{x})\mathscr{G}_\lambda(\boldsymbol{x},\sigma^2)\,\mathrm{d}\boldsymbol{x}$. The first two lemmas are concerned with the case where $p(\boldsymbol{x})$ is a much narrower distribution than $\mathscr{G}_\lambda(\boldsymbol{x},\sigma^2)$. Lemma 1 states that in such cases one can approximate the integral by replacing $p(\boldsymbol{x})$ by a Gaussian distribution with the same first- and second-order moments.

LEMMA 1. *Let $p(\boldsymbol{x})$ be a p.d.f. with mean $\boldsymbol{m}_1$, second- and third-order central moments $\boldsymbol{m}_2$ and $\boldsymbol{m}_3$, and absolute third- and fourth-order central moments (i.e. $\int p(\boldsymbol{x})|\boldsymbol{x}-\boldsymbol{m}_1|^3\,\mathrm{d}\boldsymbol{x}$ and $\int p(\boldsymbol{x})|\boldsymbol{x}-\boldsymbol{m}_1|^4\,\mathrm{d}\boldsymbol{x}$) l_3 and l_4. Then $\int p(\boldsymbol{x})\mathscr{G}_\lambda(\boldsymbol{x},\sigma^2)\,\mathrm{d}\boldsymbol{x} = \mathscr{G}_\lambda(\boldsymbol{m}_1,\sigma^2\boldsymbol{I}+\boldsymbol{m}_2)+\epsilon$ where*

$|\epsilon| < Kl_3/\sigma^{\lambda+3}$ for some constant K (which is the same for all p and σ). If also $\mathbf{m}_3$ is zero, then $|\epsilon| < K_1 l_4/\sigma^{\lambda+4}$ for some constant K_1 (which is the same for all p and σ).

Lemma 2 is concerned with the change in the integral when $p(\boldsymbol{x})$ has zero mean and is perturbed slightly by an expansion/contraction. The change is equal, to leading order, to that obtained if $p(\boldsymbol{x})$ is replaced by a Gaussian distribution with the same second-order moments.

LEMMA 2. *Let $p(\boldsymbol{x})$ be a p.d.f. with mean zero, second-order central moment $\mathbf{m}_2$ and absolute fourth-order central moment l_4. Also let a and h be related by $a = 1+h$. Then $p(\boldsymbol{x}/a)/a$, a p.d.f. with the same shape as p but with a different scale, satisfies*

$$\int \frac{p(\boldsymbol{x}/a)}{a} \mathscr{G}_\lambda(\boldsymbol{x}, \sigma^2)\,\mathrm{d}\boldsymbol{x} = \int p(\boldsymbol{x}) \mathscr{G}_\lambda(\boldsymbol{x}, \sigma^2)\,\mathrm{d}\boldsymbol{x} - h\frac{tr(\hat{\mathbf{m}}_2)}{\sigma^2}\mathscr{G}_\lambda(0, \sigma^2) + \epsilon$$

where

$$|\epsilon| < K\frac{hl_4}{\sigma^{\lambda+4}} + K_1\frac{h^2 tr(\hat{\mathbf{m}}_2)}{\sigma^{\lambda+2}}$$

for some constants K and K_1 (which are the same for all p and σ).

Lemmas 3 and 4 are concerned with the case where $p(\boldsymbol{x})$ is a much broader distribution than $\mathscr{G}_\lambda(\boldsymbol{x}, \sigma^2)$. Lemma 3 states that in such cases one can evaluate the integral to leading order by replacing $\mathscr{G}_\lambda(\boldsymbol{x}, \sigma^2)$ by an appropriate delta function.

LEMMA 3. *Let $p(\boldsymbol{x})$ be a p.d.f. with $\int p(\boldsymbol{x})\,\mathrm{d}\tilde{\boldsymbol{x}}$ a continuous and bounded function of $\hat{\boldsymbol{x}}$. Then $\int p(\boldsymbol{x})\mathscr{G}_\lambda(\boldsymbol{x}, \sigma^2)\,\mathrm{d}\boldsymbol{x} \to \int p(\boldsymbol{x})\,\mathrm{d}\tilde{\boldsymbol{x}}|_{\hat{\boldsymbol{x}}=0}$ as $\sigma \to 0$.*

Lemma 4 is concerned with the change in the integral when $p(\boldsymbol{x})$ has zero mean and is perturbed slightly by an expansion/contraction. The change is equal, to leading order, to that obtained if $\mathscr{G}_\lambda(\boldsymbol{x}, \sigma^2)$ is replaced by an appropriate delta function.

LEMMA 4. *Let $p(\boldsymbol{x})$ be a p.d.f. with zero mean and with $\int p(\boldsymbol{x})\,\mathrm{d}\tilde{\boldsymbol{x}}$ a continuous and bounded function of $\hat{\boldsymbol{x}}$. Also let a and h be related by $a = 1+h$. Then $p(\boldsymbol{x}/a)/a$, a p.d.f. with the same shape as p but with a different scale, satisfies*

$$\frac{1}{h}\left(\int \frac{p(\boldsymbol{x}/a)}{a}\mathscr{G}_\lambda(\boldsymbol{x}, \sigma^2)\,\mathrm{d}\boldsymbol{x} - \int p(\boldsymbol{x})\mathscr{G}_\lambda(\boldsymbol{x}, \sigma^2)\,\mathrm{d}\boldsymbol{x}\right) \to -\lambda \int p(\boldsymbol{x})\,\mathrm{d}\tilde{\boldsymbol{x}}|_{\hat{\boldsymbol{x}}=0}$$

as $(\sigma, h) \to 0$.

A sketch of the proof of these lemmas is as follows. For lemma 1 the error term ϵ can be written as $\int q'(\hat{\boldsymbol{x}})\mathscr{G}_\lambda(\hat{\boldsymbol{x}} + \hat{\boldsymbol{m}}_1, \sigma^2)\,\mathrm{d}\hat{\boldsymbol{x}}$ where $q'(\hat{\boldsymbol{x}}) = \int p(\boldsymbol{x} + \boldsymbol{m}_1)\,\mathrm{d}\tilde{\boldsymbol{x}} - \mathscr{G}_\lambda(\hat{\boldsymbol{x}}, \hat{\boldsymbol{m}}_2)$. q' reflects the non-Gaussianity of p. ϵ can then be bounded by expanding $\mathscr{G}_\lambda(\hat{\boldsymbol{x}} + \hat{\boldsymbol{m}}_1, \sigma^2)$ in a Taylor series in $\hat{\boldsymbol{x}}$. For lemma 2, the substitution $\boldsymbol{x}' = \boldsymbol{x}/a$ can be made and $\mathscr{G}_\lambda(\hat{\boldsymbol{x}}'(1+h), \sigma^2)$ expanded in a Taylor series in h. Lemma 3 is a consequence of the fact that the measure with density $\mathscr{G}_\lambda(\hat{\boldsymbol{x}}, \sigma^2)$ converges weakly (or narrowly) to a measure of mass 1 concentrated at $\hat{\boldsymbol{x}} = 0$ as $\sigma \to 0$. For lemma 4, the substitution $\boldsymbol{x}' = \boldsymbol{x}/a$ can be made and $\mathscr{G}_\lambda(\hat{\boldsymbol{x}}'(1+h), \sigma^2)/\mathscr{G}_\lambda(\hat{\boldsymbol{x}}', \sigma^2)$ expanded for small h followed by consideration of the weak limits of the measures with densities $\mathscr{G}_\lambda(\hat{\boldsymbol{x}}, \sigma^2)|\hat{\boldsymbol{x}}|^2/\sigma^2$ and $\mathscr{G}_\lambda(\hat{\boldsymbol{x}}, \sigma^2)|\hat{\boldsymbol{x}}|^4/\sigma^4$.

The integral in equations (6) and (7) can now be evaluated straightforwardly using the lemmas above (and assuming the weak condition required in lemmas 3 and 4, namely that $\int p_\Delta(\boldsymbol{x})\,\mathrm{d}\tilde{\boldsymbol{x}}$ is continuous and bounded). First we consider the cases where p_Δ is much narrower than $\mathscr{G}_\lambda(\boldsymbol{x}, \sigma_0^2)$, i.e. cases where $d \ll \sigma_0$. These are the cases which, in figure 4, lie below the left-to-right line through the figure. The required integrals

for various values of Δ are illustrated schematically in figure 3(*a*). The results follow from lemma 2 for $0 < \Delta \ll \sigma_\Delta$ and from lemma 1 for other values of Δ. Now consider the cases where p_Δ is much broader than $\mathscr{G}_\lambda(\boldsymbol{x}, \sigma_0^2)$, i.e. cases where $\sigma_0 \ll d$. These are the cases which, in figure 4, lie above the left-to-right line through the figure. The required integrals for various values of Δ are illustrated schematically in figure 3(*b*). The results follow from lemma 4 for $0 < \Delta \ll \sigma_\Delta$ and from lemma 3 for other values of Δ.

REFERENCES

BATCHELOR, G. K. 1952 Diffusion in a field of homogeneous turbulence II. The relative motion of particles. *Proc. Camb. Phil. Soc.* **48**, 345–362.

DURBIN, P. A. 1980 A stochastic model of two-particle dispersion and concentration fluctuations in homogeneous turbulence. *J. Fluid Mech.* **100**, 279–302.

EGBERT, G. D. & BAKER, M. B. 1984 Comments on paper 'The effect of Gaussian particle-pair distribution functions in the statistical theory of concentration fluctuations in homogeneous turbulence' by B. L. Sawford. *Q. J. R. Met. Soc.* **110**, 1195–1199.

GIFFORD, F. 1959 Statistical properties of a fluctuating plume dispersion model. *Adv. Geophys.* **6**, 117–137.

GRIFFITHS, R. F. 1991 The use of probit expressions in the assessment of acute population impact of toxic releases. *J. Loss Prev. Process Ind.* **4**, 49–57.

GRIFFITHS, R. F. & HARPER, A. S. 1985 A speculation on the importance of concentration fluctuations in the estimation of toxic response to irritant gases. *J. Hazard. Mater.* **11**, 369–372.

GRIFFITHS, R. F. & MEGSON, L. C. 1984 The effect of uncertainties in human toxic response on hazard range estimation for ammonia and chlorine. *Atmos. Environ.* **18**, 1195–1206.

HERRING, J. R., SCHERTZER, D., LESIEUR, M., NEWMAN, G. R., CHOLLET, J. P. & LARCHEVÊQUE, M. 1982 A comparative assessment of spectral closures as applied to passive scalar diffusion. *J. Fluid Mech.* **124**, 411–437.

KRAICHNAN, R. H. 1966 Dispersion of particle pairs in homogeneous turbulence. *Phys. Fluids* **9**, 1937–1943.

LARCHEVÊQUE, M., CHOLLET, J. P., HERRING, J. R., LESIEUR, M., NEWMAN, G. R. & SCHERTZER, D. 1980 Two-point closure applied to a passive scalar in decaying isotropic turbulence. In *Turbulent Shear Flows 2* (ed. L. J. S. Bradbury). Springer.

LARCHEVÊQUE, M. & LESIEUR, M. 1981 The application of eddy-damped Markovian closures to the problem of dispersion of particle pairs. *J. Méc.* **20**, 113–134.

LESIEUR, M. 1987 *Turbulence in Fluids*. Martinus Nijhoff.

MONIN, A. S. & YAGLOM, A. M. 1971 *Statistical Fluid Mechanics*, vol 1. MIT Press.

MONIN, A. S. & YAGLOM, A. M. 1975 *Statistical Fluid Mechanics*, vol 2. MIT Press.

MYLNE, K. R., DAVIDSON, M. J. & THOMSON, D. J. 1996 Concentration fluctuation measurements in tracer plumes using high and low frequency response detectors. *Boundary-Layer Met.* (to appear).

RICHARDSON, L. F. 1926 Atmospheric diffusion shown on a distance-neighbour graph. *Proc. R. Soc. Lond.* A **110**, 709–737.

SAWFORD, B. L. 1983 The effect of Gaussian particle-pair distribution functions in the statistical theory of concentration fluctuations in homogeneous turbulence. *Q. J. R. Met. Soc.* **109**, 339–354.

SAWFORD, B. L. & HUNT, J. C. R. 1986 Effects of turbulence structure, molecular diffusion and source size on scalar fluctuations in homogeneous turbulence. *J. Fluid Mech.* **165**, 373–400.

THOMSON, D. J. 1987 Criteria for the selection of stochastic models of particle trajectories in turbulent flows. *J. Fluid Mech.* **180**, 529–556.

THOMSON, D. J. 1990 A stochastic model for the motion of particle pairs in isotropic high-Reynolds-number turbulence, and its application to the problem of concentration variance. *J. Fluid Mech.* **210**, 113–153.

TOWNSEND, A. A. 1954 The diffusion behind a line source in homogeneous turbulence. *Proc. R. Soc. Lond.* A **224**, 487–512.